Drainage of Cerebral Abscesses Prior to Valve Replacement in Stable Patients with Acute Left-Sided Infective Endocarditis

Adrian Molnar[1], Ruxandra Beyer[2], Stefan Florian[3], Dafin Fior Mureşanu[*,4,5], Catalin Trifan[6], Ioan Mureşan[6], Diana Săcui[6], Traian Scridon[6] and Radu N. Bălănescu[7]

[1]*Cardiovascular Surgery Clinic, Heart Institute, Cluj-Napoca, Romania*

[2]*Cardiology Clinic, Heart Institute, Cluj-Napoca, Romania*

[3]*Neurosurgery Clinic, Cluj-Napoca County Hospital, Cluj-Napoca, Romania*

[4]*Department of Clinical Neurosciences, University of Medicine and Pharmacy "Iuliu Haţieganu", Cluj-Napoca, Romania*

[5]*RoNeuro" Institute for Neurological Research and Diagnostic, Cluj-Napoca, Romania*

[6]*Cardiovascular Surgery Clinic, Heart Institute, Cluj-Napoca, Romania*

[7]*Department of Pediatric Surgery, "Grigore Alexandrescu" Emergency Clinical Hospital for Children, Bucharest, Romania*

Dafin Fior Mureşanu

Abstract: Despite the medical and surgical advancements in the treatment of patients with acute infective endocarditis (IE), neurologic complications remain problematic. They can arise through various mechanisms consisting of stroke or transient ischemic attack, cerebral hemorrhage, mycotic aneurysm, meningitis, cerebral abscess, or encephalopathy. Most complications occur early during the course of IE and are characteristic to left-sided pathology of native or prosthetic valves. We present a case of a 46 year old male patient who presented to our clinic with mitral valve IE caused by coagulase negative staphylococcus. Although under correct antibiotic treatment, he continued to be feverish and started to present unspecific neurological symptoms (amnesia, confusion, asthenia and general malaise). The cerebral magnetic resonance imaging (MRI) revealed multiple cerebral abscesses. Because the patient was hemodynamically stable we decided to address the cerebral abscess first and the cardiac lesion second. The patient made a full recovery after undergoing antibiotic treatment and surgical procedures of drainage of the cerebral abscess and mitral valve replacement. After reviewing the literature regarding the management of patients with IE and cerebral complications and based on this particular case, we conclude that in select cases of stable patients with cerebral abscess and IE, the neurological lesion should always be addressed first and cardiac surgery should be performed second.

Keywords: Cardiac surgery, cerebral abscess, endocarditis, neurological complications, neurosurgery, valve replacement.

This special number is dedicated to the *Editorial Advisory Board Members* of *CNS & Neurological Disorders-Drug Targets* who have been a constant source of knowledge and inspiration to the journal's readership.

INTRODUCTION

The diagnosis and treatment of infective endocarditis (IE) in the modern countries has changed dramatically over the past 35 years [1, 2], but the prevalence remains unchanged and annual mortality approaches 40% [1]. The incidence of IE is approximately 1.7-6.2 cases per 100 000 patient years, although numbers are bigger in cohorts which are at risk as are intravenous drug users [1, 2]. Men are more at risk than women are (in a ratio of 2: 1), and because of higher prevalence of degenerative valve disease, the incidence progressively increases with age. However, in one French study 47% of patients with IE had no discernable previous cardiac disorder [3]. The relation to dental procedures is no longer as emphasized as in the past, and IE is more likely to develop in patients with previous valvular surgery or in the context of iatrogenic or nosocomial infection [4].

Despite the availability of a wide range of antibiotics, IE continues to be a major problem globally. The primary reasons include the presence of extra-cardiac complications of which central nervous system (CNS) involvement is possibly the most serious [5]. The association between infective endocarditis and neurological complications (NC) has been recognized more than a century ago, when Sir William Osler first stated that the association between fever, heart murmur, and hemiplegia points towards infectious endocarditis [6].

In approximately 10% to 15% of patients with IE, the nervous system exhibits the first signs, often before the beginning of any treatment [7]. Presently IE is one of the

*Address correspondence to this author at the Department of Clinical Neurosciences, University of Medicine and Pharmacy "Iuliu Haţieganu", Victor Babeş Street No. 8, 400012 Cluj-Napoca, Romania;
Tel: +4 0724 35 30 60, Ext. 2116; Fax: +4-0264-406845, +4-0264-597256;
E-mail: dafinm@ssnn.ro

1871-5273/15 $58.00+.00

biggest causes of acute cerebral infarction in young people [8]. Autopsy findings performed on patients with IE have demonstrated the following types of central nervous system (CNS) lesions: cerebral infarction (65-68%), hemorrhage (35-57%), abscess (10-31%) and focal meningitis (5-14%) [5]. Reports have indicated that there is a daily risk of stroke of 0.5% in patients with IE [7].

The incidence of NC in acute IE is dependent on the infective organism and the valvular location of the infection. The highest incidence of NC has been reported in patients with *Staphylococcus aureus* vegetations of the mitral valve (87%) [9]. The mortality rate in the first phase of the disease is three times higher for patients infected with Staphylococcus compared to those infected with other microorganisms (34% *vs* 10%) [9]. This risk factor is independent of the patient's age, co-morbidities or other usual prognosis factors, therefor denoting the necessity for early administration of aggressive treatment [10].

The medical and surgical management of IE that is complicated by any neurological disorder, and most importantly the timing of cardiac surgery in these patients are topics of international debate. Most of the patients with a NC also meet at least one other criteria that make them candidates for cardiac surgery [11]. Natural concerns arise when speaking about the part surgery plays in these particular circumstances. Neurological deterioration is a possibility and also intra- or post-operative cerebral bleeding might occur. The risks are negligible after an asymptomatic cerebral embolism or transient ischemic attack [11] and heart surgery in extra-corporeal circulation may be performed safely and given the indication is made, without delay. Provided that acute CNS hemorrhage is excluded and the patient's neurological status is not severe (deep coma), the existing indications for emergency surgery still apply: congestive heart failure, infection that doesn't respond to treatment, presence of heart abscess, or the persistence of a high embolic risk. Cardiac surgery can be performed in these situations with low risk of neurological deterioration (cerebral bleeding, oedema or coma) (3% to 6%) [12]. Neurological prospect is worse in the presence of intracranial hemorrhage; in these cases cardiac surgery should be put off for at least 30 days [13, 14]. The timing of cardiac surgery in patients with IE and cerebral abscess is however unclear. We present our successful management of such a case and a review of the literature that helped us with decision making.

CASE REPORT

A 47 year old man presented to his general practitioner complaining of fever and malaise that had started 4 days before. He had no cardio-vascular priors and an unimpressive medical history. He self-medicated with a combination of antipyretics (ibuprofen 200mg three times a day) and antibiotics (amoxicillin 500mg two time a day), but found no improvement. Finding no clinical signs of respiratory infection he referred the patient to the infectious disease clinic for further investigations. Blood cultures harvested there demonstrated a coagulase negative staphylococcus bacteremia and the cardiac ultrasound showed severe mitral regurgitation with a relatively large vegetation on posterior mitral valve. The diagnosis was acute IE of the mitral valve, and antibiotic treatment was initiated. He was transferred to our clinic 6 days after.

On admission to our hospital he was hemodynamically stable, with no clinical signs of severe cardiac failure, and with normal renal and pulmonary functions. He did however exhibit signs of sinus tachycardia, fever that reached 39°C and skin lesions characteristic of septic emboli. He had previously received a double association of antibiotic vancomycin and meropenem according to the antibiogram results. A third drug - doxycycline was introduced after demonstrating positive serology for *Mycoplasma pneumoniae*. Three days into the treatment we decided to cease the administration of meropenem because of elevated seric levels of liver enzymes. We performed transesophageal echocardiography which revealed severe mitral regurgitation on a myxomatous valve with multiple chordae ruptures, cusp

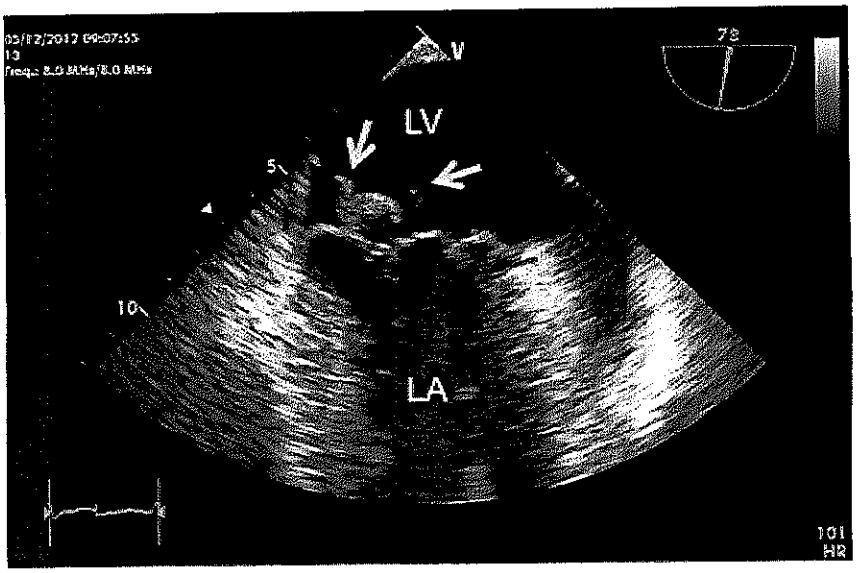

Fig. (1). Myxomatous mitral valve with endocarditis. Transesophageal echocardiography views: posterior leaflet thickening with flail of the P2-segment (ruptured chordae tendineae) and vegetation on the atrial surface of the leaflet (arrows) in systole.

rupture and a 5x6 mm vegetation attached to the posterior mitral valve (Fig. **1**), as well as a left ventricle with normal systolic function, slightly dilated, with no signs of important pulmonary hypertension.

Although under a correct therapy of antibacterial medication, the patient continued to present high fever, general malaise and asthenia 8 day into the course of the treatment. Furthermore he began to exhibit signs of neurological dysfunction - amnesia, confusion. He also presented consistently elevated inflammatory blood test results (C-reactive protein - 140.43 mg/L (normal: 0-5mg/L), erythrocyte sedimentation rate - 110 mm, white cell blood count - 34000/μL). Under the suspicion of a secondary neurological infective process, we performed a cerebral magnetic resonance imaging (MRI) which showed multiple sub-centimeter cerebral abscesses localized in the supratentorial region (corpus callosum, diencephalon) and two larger abscesses in the occipital area (Fig. **2**). A joint team comprising a cardiac surgeon, a neurosurgeon and an infectious disease specialist assessed the patient and decided to first treat the cerebral complication first and surgically address the cardiac lesions second. After correction of a severe thrombocytopenia by administration of thrombocyte concentrate, the neurosurgical team performed the evacuation of the occipital abscesses. The intervention was successful, as shown in the post-operative cerebral CT (Fig. **3**), and the patient recovered.

After his release from the neurosurgical clinic, the patient was admitted to the infectious disease clinic for continued treatment. During the next 4 weeks the patient remained stable and was able to complete a six week antibacterial treatment. The fever disappeared, the white blood count normalized and the level of systemic inflammation decreased.

We transferred the patient to our clinic. The control echocardiography showed severe mitral regurgitation, an enlarged left atrium, normal left and right ventricular function, and mild pulmonary hypertension. Our team decided to perform a mitral valve replacement procedure. We performed a coronary angiogram which revealed no significant coronary lesions.

Surgery was performed with the patient under general anesthesia and in a supine position. After a median sternotomy, the pericardium was opened longitudinally. After heparinization, extra-corporeal circulation was established between the two venae cavae and the ascending aorta. A cross clamp was placed on aorta and by anterograde

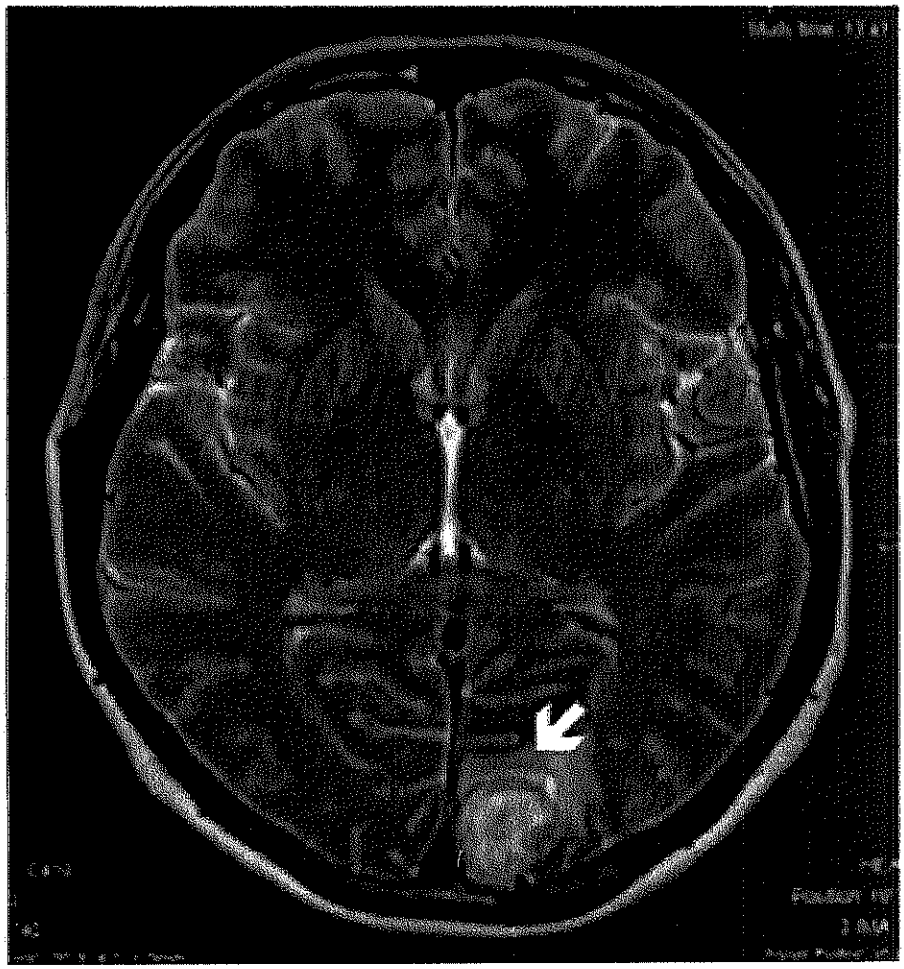

Fig. (2). Cerebral abscesses – contrast MRI: T2 axial section, which shows a formation localized intraaxialy, on the periphery of the left occipital lobe, well delineated, of approximately 20 mm with T2 hypersignal, with perilesional oedema.

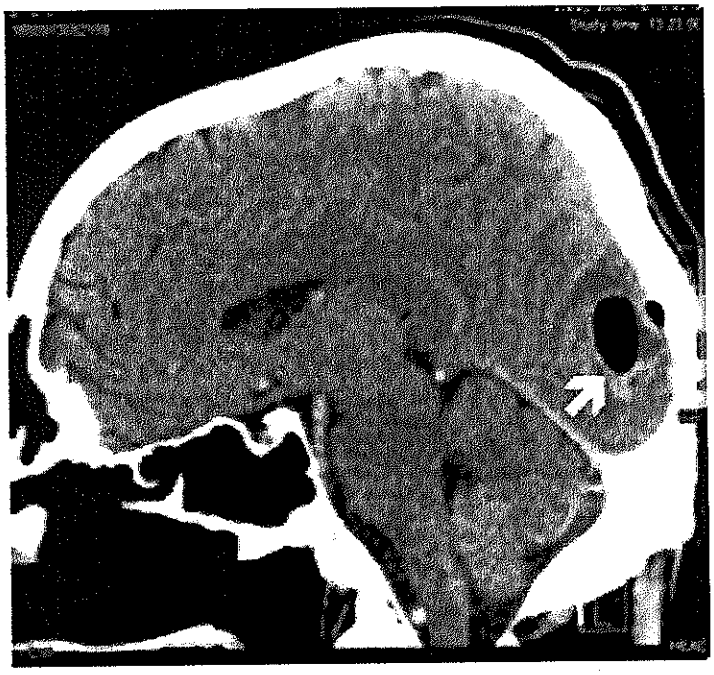

Fig. (3). Multiplanar sagittal reconstruction after cerebral computed tomography: air-filled cavity, secondarry to abscess evacuation (arrow).

intermittent hypothermic blood cardioplegia from the aortic root, cardiac arrest was established. Hypothermia was moderate (28°C). The mitral valve was approached *via* a standard left atriotomy parallel to the interatrial sulcus. An atrium retractor was positioned for optimal exposure. Upon inspection we encountered an evacuated abscess involving the posterior aspect of the mitral annulus, a small 5 mm vegetation on the posterior mitral valve, ruptured chordae, but no sign of an active infectious process. From the ventricular side, the aortic valve was normal, and there were no associated cardiac lesions. After removal of the native mitral valve (fragments were sent to the laboratory for histological and microbiological analyses) a mechanical valve was mounted (29 mm, ATS Medical manufactured by Medtronic, Inc., Minneapolis, MN, United States of America) with pledgeted sutures. The left atrium was closed, the heart de-aired, started and afterwards easily weaned from cardio-pulmonary by-pass with only a continuous infusion of 2μg/kg/min of dobutamine for inotropic support.

After a short 2 day stay in the intensive care unit (normal thoracic drainage, and mild inotropic support) the patient made a good recovery. The antibiotic treatment was continued for 7 more days after the surgery, until bacteriological results confirmed that the valve was sterile. The patient was released 9 days after surgery. The patient remained symptom-free from a neurological and cardiac point of view at the 1, 3 and 6 month follow-up exams and the echocardiographic control showed normal functioning valve prosthesis.

DISCUSSION

In Western European populations, chronic rheumatic heart disease is more and more rare, whereas degenerative valve disease in elderly people, intravenous drug abuse, previous valve surgery, or vascular catherisation have become increasingly frequent, together with a rise in frequency of staphylococcal infections or those due to other fastidious micro-organisms. Even worse is that, new pathogens are being identified as cause of the infection, and multidrug resistant germs challenge standard drug regimens [1]. In the pre-antibiotic era, the mortality rate of infective endocarditis was nearly 100%. The current mortality rate of 20-50% is attributed to congestive heart failure or acute valve regurgitation [4]. Studies have shown that the mortality rate is higher in patients with CNS involvement (58-74%) compared to patients without CNS involvement (20-56%) [4].

Macroscopic brain abscess is a rare complication of bacterial endocarditis, and there is little if any available medical data concerning how to manage these patients but most importantly the timing of the neurosurgical and cardiac interventions. We present a case of left-sided bacterial endocarditis complicated by a large cerebral abscess. Because the patient was stable we decided to drain the brain abscess first, complete the antibiotic treatment, and only afterword resolve the cardiac lesions. The patients evolution was good, his recovery fast and he remained symptom- free from a neurological and cardiac point of view.

Systemic emboli might occur in up to 50% of patients with IE [15, 16]. The CNS is the most frequent target, in 65% of embolic events; about 90% of these affect the territory supplied by the middle cerebral artery [16]. In up to 25% of cases embolic complications may be clinically silent [17, 18]. If present the symptoms might vary, and can range from mild confusion to deep coma. More recent studies have shown a rather polymorph pattern of NC attributed to the advancement in age of the patients and the increased number of nosocomial infections and intravenous drug users [3]. If present, the neurological syndrome is often the first clinical feature in endocarditis and the most frequent neurological

complication is cerebral ischemia. In patients with clinical signs ischemic stroke and those with intracranial bleeding, auscultation of a heart murmur and systemic signs of infection point to endocarditis. Encephalopathy in endocarditis is for the most part attributable to cerebral infarction. In bacterial meningitis or cerebral abscess an unusual isolate should arise suspicion [19].

Emboli cause cerebral infarction, but also lead to the development of mycotic aneurysms, cerebral abscesses, and also meningitis. Miliary microscopic abscesses are more common than large abscesses, predominantly in patients with an acute form of the disease and miliary dissemination in other parts of the body [20]. Two features influence the incidence of NC: (1) the site of endocarditis with 76% of NC occurring in patients with mitral valve endocarditis compared to 37% incidence of NC in other cases, and (2) the infecting organism: NC have an incidence of 71% in patients with S. aureus endocarditis *versus* only 45% in patients with endocarditis caused by other bacteria [21]. The highest rate of embolic complications is seen in left-sided IE, especially when infection is related to *Staphylococcus aureus*, Candida, HACEK and *Abiotrophia* organisms [22]. Our patient had positive blood cultures for coagulase negative staphylococcus, but also positive serology for *Mycoplasma pneumoniae*, and received treatment for both. Staphylococcal endocarditis most often occurs in patients who suffer from chronic kidney failure, diabetes mellitus, alcoholism, cancer, immune suppression and drug abuse. Their prognosis is worse and their clinical signs appear and evolve rapidly, thus necessitating early hospital admission [7, 9].

Embolic complications usually occur before the diagnosis is set or within 2 weeks thereafter. Concerning the timing of surgery, several studies have stated that embolic risk decreases radically during the first 2 to 3 weeks of successful drug therapy [18, 22, 23]. Data from the International Collaboration on Endocarditis proved that the frequency of stroke decreases form 4.8/1000 patient-days during the first week of therapy to 1.7/1000 patient-days in the second week under correct antibacterial drug therapy [23]. In our case the neurological symptoms appeared after the first week, but we suspect that the embolic event occurred well before that. This is supported by (1) the nature of the complication - an abscess takes time to form, and (2) the size of the abscess.

Several echocardiographic and clinical parameters have been proven to by predictive factors associated with greater risk of embolism: size and mobility of vegetations, location on the mitral valve, increasing size under correct antibiotic therapy, Staphylococcal infection, history of earlier embolism [23-27]. The optimal timing of cardiac surgery after an ischemic stroke is not yet well established, due to lack evidence provided by controlled studies. Therefore, it is yet unclear at what time a valve procedure should be performed in patients with IE and NC, particularly in patients with IE and cerebral abscess.

We based our decision to postpone the cardiac intervention in favor of the neurosurgical intervention on several aspects. (i) The patient didn't respond well to antibiotic treatment suited for the responsible bacteria and we attributed this to the lack of penetration of the medication into the abscess. (ii) The patient was stable, with no signs of severe cardiac failure. (iii) The abscess was already large and, if it increased, might cause further neurological damage. (iv). The vegetation was relatively small, and did not increase in time. (v) The medical data we found was insufficient concerning the timing of cardiac surgery in patients with IE and cerebral abscess.

Surgery already has an established role in the management of IE across a wide range of patients, a role that increases as the complexity of patients with this difficult condition rises. Concerning only an isolated case, our data is of course insufficient to establish a protocol for the management of patients with IE and cerebral abscess. Large international collaborations should provide us a more robust evidence base to guide treatment strategies in patients with IE and cerebral abscess. Nevertheless, decision making in individual patients will remain difficult, with the best outcomes obtained as a result of expert multidisciplinary collaboration between the cardiologist, microbiologist, neurologist, and cardiac surgeon. Only with such interaction will the questions of "whom?" and "when?" become answerable.

CONCLUSION

It is yet unestablished how to manage patients with IE and cerebral abscess, but we consider that the drainage of a large cerebral abscess prior to valve replacement surgery is the correct way to handle these patients. In our case it yielded very good results, but further studies are necessary in order to create a usable treatment protocol.

LIST OF ABBREVIATIONS

CNS = Central nervous system

CT = Computed tomography

IE = Infective endocarditis

MRI = Magnetic resonance imaging

NC = Neurological complications

CONFLICT OF INTEREST

The authors confirm that this article content has no conflict of interest.

ACKNOWLEDGEMENTS

Declared none.

REFERENCES

[1] Cabell CH, Jollis JG, Peterson GE, *et al.* Changing patient characteristics and the effect on mortality in endocarditis. Arch Intern Med 2002; 162: 90-4.

[2] Prendergast BD. The changing face of infective endocarditis. Heart 2006; 92: 879-85.

[3] Garg N, Kandpal B, Garg N, *et al.* Characteristics of infective endocarditis in a developing country—clinical profile and outcome in 192 Indian patients, 1992-2001. Int J Cardiol 2005; 98: 253-60.

[4] Bouza E, Menasalvas A, Munoz P, *et al.* Infective endocarditis—a prospective study at the end of the twentieth century: new

predisposing conditions, new etiologic agents, and still a high mortality. Medicine 2001; 80: 298-307.

[5] Patel FM, Das A, Banerjee AK. Neuropathological complications of infective endocarditis: study of autopsy material. Neurology 2001; 49: 41-6.

[6] Osler W. Gulstonian lectures on malignant endocarditis. Lancet 1885; 1: 415-8.

[7] Corral I, Martín-Dávila P, Fortún J, *et al.* Trends in neurological complications of endocarditis. J Neurol 2007; 254: 1253-9.

[8] Santoshkumar B, Radhakrishnan K, Balakrishnan KG, Sarma PS. Neurologic complications of infective endocarditis observed in a south Indian referral hospital. J Neurol Sci 1996; 137(2): 139-44.

[9] Kanter MC, Hart RG. Neurologic complications of infective endocarditis. Neurology 1991; 41(7): 1015-20.

[10] Roder BL, Wandall DA, Espersen F. Neurologic manifestations in Staphylococcus aureus endocarditis: a review of 260 bacteremic cases in nondrug addicts. Am J Med 1997; 102(4): 379-86.

[11] Hart RG, Foster JW, Luther MF, Kanter MC. Stroke in infective endocarditis. Stroke 1990; 21(5): 695-700.

[12] Ruttmann E, Willeit J, Ulmer H, *et al.* Neurological outcome of septic cardioembolic stroke after infective endocarditis. Stroke 2006; 37: 2094-9.

[13] Eishi K, Kawazoe K, Kuriyama Y, Kitoh Y, Kawashima Y, Omae T. Surgical management of infective endocarditis associated with cerebral complications: multi-center retrospective study in Japan. J Thorac Cardiovasc Surg 1995; 110: 1745-55.

[14] Gillinov AM, Shah RV, Curtis WE, *et al.* Valve replacement in patients with endocarditis and acute neurologic deficit. Ann Thorac Surg 1996; 61: 1125-9.

[15] Thuny F, Disalvo G, Belliard O, *et al.* Risk of embolism and death in infective endocarditis: prognostic value of echocardiography: a prospective multicenter study. Circulation 2005; 112: 69-75.

[16] Heiro M, Nikoskelainen J, Engblom E, Kotilainen E, Marttila R, Kotilainen P. Neurologic manifestations of infective endocarditis: a 17 year experience in a teaching hospital in Finland. Arch Intern Med 2000; 160: 2781-7.

[17] Di Salvo G, Habib G, Pergola V, *et al.* Echocardiography predicts embolic events in infective endocarditis. J Am Coll Cardiol 2001; 37: 1069-76.

[18] Thuny F, Avierinos JF, Tribouilloy C, *et al.* Impact of cerebrovascular complications on mortality and neurologic outcome during infective endocarditis: a prospective multicenter study. Eur Heart J 2007; 28: 1155-61.

[19] Angstwurm K, Borges AC, Halle E, Schielke E, Weber JR. Neurological complications of infective endocarditis. Nervenarzt 2004; 75(8): 734-41.

[20] Pruitt AA, Rubin RH, Karchmer AW, Duncan GW. Neurologic complications of bacterial endocarditis. Medicine (Baltimore) 1978; 57(4): 329-43.

[21] Le Cam B, Guivarch G, Boles JM, Garre M, Cartier F. Neurologic complications in a group of 86 bacterial endocarditis. Eur Heart J 1984; 5(Suppl C): S97-100.

[22] Vilacosta I, Graupner C, San Román JA, Sarriá C, Ronderos R, Fernández C. Risk of embolization after institution of antibiotic therapy for infective endocarditis. J Am Coll Cardiol 2002; 39: 1489-95.

[23] Dickerman SA, Abrutyn E, Barsic B, *et al.* The relationship between the initiation of antimicrobial therapy and the incidence of stroke in infective endocarditis: an analysis from the ICE Prospective Cohort Study (ICE-PCS). Am Heart J 2007; 154: 1086-94.

[24] Rohmann S, Erbel R, Görge G, *et al.* Clinical relevance of vegetation localization by transoesophageal echocardiography in infective endocarditis. Eur Heart J 1992; 13: 446-52.

[25] Sanfilippo AJ, Picard MH, Newell JB, *et al.* Echocardiographic assessment of patients with infectious endocarditis: prediction of risk for complications. J Am Coll Cardiol 1991; 18: 1191-9.

[26] Rohmann S, Erbel R, Darius H, *et al.* Prediction of rapid *versus* prolonged healing of infective endocarditis by monitoring vegetation size. J Am Soc Echocardiogr 1991; 4: 465-74.

[27] Mugge A, Daniel WG, Frank G, Lichtlen PR. Echocardiography in infective endocarditis: reassessment of prognostic implications of vegetation size determined by the transthoracic and transesophageal approach. J Am Coll Cardiol 1989; 14: 631-8.

Received: August 8, 2014 **Revised: January 19, 2015** **Accepted: January 19, 2015**

Case report

Med Ultrason 2016, Vol. 18, no. 2, 253-256
DOI: 10.11152/mu.2013.2066.182.ttr

The value of transthoracic and transesophageal echocardiography for the diagnosis of the native aortic infective endocarditis valve complications: a case report and literature review.

Adrian Molnar[1], Diana Sacui[1], Simona Manole[2], Amanda Radulescu[3], Ruxandra Beyer[4]

[1]Cardiovascular Surgery Department, Heart Institute, [2]Radiology Clinic, Emergency Clinic County Hospital, [3]Infectious Disease Clinic, [4]Cardiology Department, Heart Institute, Cluj-Napoca, Romania

Abstract

Despite its current limitations transthoracic echocardiography is still widely used for the anatomical and functional evaluation of patients with infective endocarditis. However, all these limitations can be overcome by using transesophageal echocardiography. We present the case of a 42-year-old male patient, diagnosed with aortic valve infective endocarditis, whose transthoracic echocardiography showed only a cusp vegetation and aortic regurgitation, but raised the suspicion of periannular complications. The transesophageal echocardiography revealed a circular aortic root abscess and a ventricular septal defect with left-to-right shunt, and consequently leads to a complete different surgical tactical approach. The patient was urgently referred for surgery due to the rapid deterioration of the hemodynamic status, and had a good outcome on the short-term follow-up.

Keywords: infective endocarditis, echocardiography, periannular complications

Introduction

Infective endocarditis (IE) remains a cardiac pathology associated with high morbidity and mortality, and furthermore a major challenge for the cardiac surgeon [1]. Despite the improving quality of life as well as the evolving diagnosis methods and antibiotic therapy, IE continues to affect a relatively large segment of the active population with an incidence of 3–10 episodes/100 000 person-years (mostly men aged between 70 and 80 years) [2-4].

Depending on the site of infection and the presence or absence of intracardiac foreign material, IE is classified as follows: left-sided native valve IE, left-sided prosthetic valve IE, right-sided IE, and device-related IE (IE developed on pacemaker or defibrillator wires, with or without the involvement of the valve). Regarding the acquisition, IE is divided into community-acquired IE, health care-associated IE (nosocomial and non-nosocomial), and IE in intravenous drug abusers (IVDAs) [2]. The new European Society of Cardiology (ESC) guidelines emphasize the role of transthoracic echocardiography (TTE) as a first line imaging study in the diagnosis of this disease (Class IB recommendation) [5].

Transesophageal echocardiography (TEE) is a non-invasive and cost-effective examination, able to comprehensively characterize the morphology and functional status of the cardiac and vascular structures affected by the infectious process. This information is essential in the setting of the surgical approach, considering that a favorable long term outcome depends on the complete removal of the infected tissue followed by the reconstruction or replacement of the excised lesions. Sometimes these excisions are widely extended, and the tissue destruction is extremely large. In these situations, the diagnostic accuracy and the magnitude of surgical reconstruction become a challenge for both the cardiologist and the cardiac surgeon such as the case we are going to presentnow.

Received 10.10.2015 Accepted 16.11.2015
Med Ultrason
2016, Vol. 18, No 2, 253-256
Corresponding author: Diana Sacui
Cardiovascular Surgery Clinic, Heart Institute
19-21, Motilor street,
400001, Cluj-Napoca, Romania
Phone: +40-264-591.941
E-mail: diana_sacui27@yahoo.com

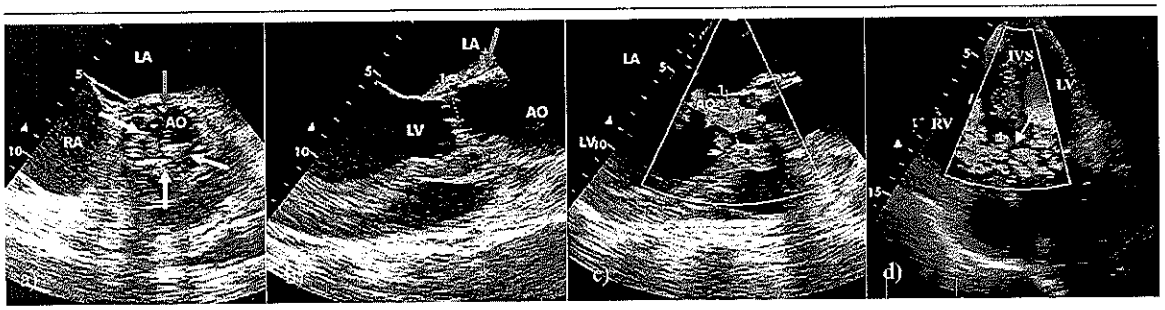

Fig 1. a) Transesophageal short axis view of the aortic valve: vegetation (inhomogeneous structures attached to the valvular tissue), perforations, retractions, and scars (white arrows) were found. In the periannular region between the aorta and left atrium an echolucent space suggests the presence of an aortic root abscess (red arrow); b) Transesophageal long axis view of the aortic valve and ascending aorta. The echolucent space located around the aortic valve annulus and proximal ascending aorta suggests a circular aortic root abscess (red arrows); c) Transesophageal long axis view of the aortic valve and ascending aorta, colour Doppler. Severe aortic regurgitation caused by a co-aptation defect of the modified and perforated cusps; d) Transthoracic echocardiography, apical 4-chamber view, colour Doppler. A colour flow from the aortic root into the right ventricle indicates a left-to-right shunt caused by a fistula between the aortic root and the right ventricle (arrow). LV: left ventricle; RV: right ventricle; IVS: interventricular septum; Ao: ascending aorta.

Case report

A 42-year-old man was admitted to our intensive care unit for dyspnea at rest and extreme malaise. The patient had a 4-week history of fever, anorexia, and 6 kg loss weight. He denied any history of travelling, prior surgery, dental procedures, or contact with animals over the previous 3 months.

One week before presentation he was admitted to the Infectious Disease Clinic. Physical examination revealed that time a dehydrated patient with hyperpyrexia (42°C), blood pressure of 80/60 mmHg and heart rate 104 beats/minute. Blood tests showed elevation of C-reactive protein to 16.7 mg/dL (normal values: <1 mg/dL), increase of the white blood cells count to 20,400/μL and normocytic anemia with a hemoglobin level of 11.8 g/dL. In all three sets of blood cultures obtained in the first hours after admission (30 minutes apart), Gram staining detected Gram-positive diplococci – *Streptococcus pneumonia* with sensitivity to penicillin G. Chest radiography revealed peribronchial reticulonodular opacity. TTE was carried out using a GE Vivid S6 echo system, which illustrated a 0.6 cm vegetation attached to the right coronary cusp of the aortic valve and moderate aortic regurgitation (vena contracta 5 mm, pressure half time PHT 550 ms, velocity time integral VTI in the descending aorta 6 cm). No periannular complications were detected.

According to Duke criteria [6], the patient was diagnosed with definite infective endocarditis; subsequently, antibiotherapy with Ceftriaxone and Gentamycin was initiated. One week after admission to the Infectious Disease Clinic, the patient had an unfavorable clinical course with an ongoing high fever, worsening of dyspnea, fatigue and hypotension, and consequently he was transferred to our emergency department. At admission the electrocardiogram revealed sinus tachycardia, right bundle branch block, and right axis deviation. The chest X-ray showed a slightly dilated left heart and pulmonary edema. Due to the high probability of periannular complications, a transesophageal echocardiography (TEE) was performed (GE Vivid S6 echo system). The bi-dimensional (2D) images identified a tricuspid aortic valve with severe endocarditic lesions: vegetation, cusp ruptures, and retractions. The echolucent space located around the aortic valve annulus and proximal ascending aorta suggested a circular aortic root abscess. Additionally, a severe aortic regurgitation (vena contracta 12 mm, PHT 160 ms, VTI in the descending aorta 20 cm) was identified. In the apical 4-chamber view a continuous color flow from the aortic root into the right ventricle indicated a perforation in the aortic wall, erosion into the right ventricle and creation of a continuous left-to-right shunt between the aortic root and the right ventricle, suggesting the presence of a fistula (fig 1). The presence of the shunt at the level of the basal interventricular septal region suggested the extension of the infectious process to the membranous septum, with an important ventricular septal defect (VSD). The left and right ventricles were enlarged (LV diameters 65/38 mm, RV diameter 45 mm below tricuspid valve), with hyperdynamic contraction and normal systolic function (LVEF 68%, TAPSE 30 mm). Also a moderate pulmonary hypertension (PASP 60 mmHg) was found. The patient was referred for emergency cardiac surgery

Intraoperatively purulent pericardial liquid and thick pericardial layers, with inflammatory changes were

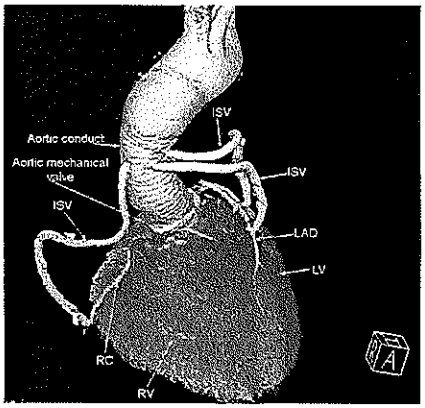

Fig 2. Cardiac computed tomography (3-D reconstruction), 1 month after surgery: aortic conduit containing a mechanical prosthesis and triple coronary artery bypass graft. All grafts are patent, without complications and without peri-prosthetic effusions or false aneurysms. ISV: internal saphenous vein; RC: right coronary (artery); RV: right ventricle; LV: left ventricle; LAD: left anterior descending (artery).

found. On the anterior aortic wall a tumor mass of approximately 4/3 cm was observed and was interpreted as an aortic root abscess. The inspection of the aortic valve revealed a 2/2 cm vegetation on the right coronary commissure, a small abscess on the left coronary commissure, and a giant abscess with a fistula opened into the right ventricle, lying between the left and right coronary ostia, with a large VSD. The muscular and the aortic walls were extremely friable, and a small fistula between the inner and the outer aortic layers on the anterior aortic wall was also noticed. The aortic intima was completely damaged, with severe inflammatory lesions at the level of the coronary ostia. The infected aortic valve and the surrounding necrotic tissue were excised. The VSD was covered with bovine pericardial patch on the inferior wall, and continuous suture of the other walls. A valved conduit containing a mechanical prosthesis of 23 mm and a tubular Dacron graft of 25 mm was inserted. The re-implantation of the coronary ostia into the tubular graft was technically not possible so a triple coronary bypass (CABG) with saphenous veins was performed. Intraoperative TEE was used to control the success of the procedure.

The overall postoperative course of the patient was uneventful. Two weeks postoperatively, TTE was repeated. The aortic mechanic prosthesis was with normal pressure gradients. There was no communication between the aortic root and heart chambers and no residual interventricular shunt. In order to evaluate the postoperative results, a CT-angiography of the aorta was performed 3 months after surgery (fig 2).

Discussions

Considering the main risk factors for IE of the native valve (increased longevity, prosthetic valves, increased exposure to nosocomial bacteremia, use of iv drugs, HIV infection, mitral valve prolapsed) [7-10] we found no risk factors for IE in our patient. As perivalvular IE is usually associated with a higher incidence of serious complications, a more complicated surgical procedure, or death, early diagnosis is essential [11]. Useful information concerning the diagnosis and the severity of IE, as well as the short- and long-term prognosis are given by TEE [12].

In our case, neither the initial nor the second TTE performed by a very experienced cardiologist were able to detect other lesions than the vegetation attached to the right coronary cusp of the aortic valve with secondary moderate aortic regurgitation. The presence of the periannular abscess and the VSD with left-to-right shunt were revealed only by the TEE. Our results are in line with literature data [13], confirming that TEE was an essential tool in our patient. In these circumstances, we can state that TEE had a conclusive role for the comprehensive preoperative diagnosis. The accuracy of the images provided by this technique was confirmed by the intraoperative findings. Moreover the ESC guideline recommends to perform TEE not only pre-operatively for diagnosis purposes, but also intraoperatively in all cases of infective endocarditis requiring surgery, due to its ability its affect at least one of the following parameters operative plan, quality control of valve repair/replacement, hemodynamic assessment or de-airing [5,14]. Precise recognition of possible complications is important for the medical and surgical management of these patients, as those complications could generate unexplained congestive heart failure and hemodynamic deterioration in some cases with aortic valve endocarditis [14]. Extension of the infection to the perivalvular tissues is a sign of poor prognosis in the evolution of the disease: it may lead to endothelial erosion, perivalvular abscess, mycotic aneurysm, and intracardiac fistulae [12]. Intraoperative findings in our patient were characterized by severe damage at the level of the aortic wall, coronary ostia and inter-ventricular septum; these supplementary lesions made the surgical technique more complicated and challenging.

The risk of recurrence among survivors of IE varies between 2.7 and 22.5% and prophylactic measures should be very strict, involving postoperative regular echocardiography control examinations (TTE, TEE) [2]. We used TEE immediately after finishing the surgical procedure and TTE two weeks post-operatively in order to have the best evaluation of our patient's outcome, besides the significant clinical improvement. These non-

invasive techniques allowed us to be confident with the complex treatment (surgical and medical) managed for this patient.

The repetition of TTE and TEE in the patients' follow-up program is extremely important, as it is stressed in the 2015 ESC guidelines: TTE is recommended at completion of antibiotic therapy for evaluation of cardiac and valve morphology and function [5].

Finally, we would like to emphasize once more the case complexity, with regard to the imaging studies (TTE, TEE, and CT-angiography), as well as regarding the surgical technique (aortic root reconstruction, ventricular septal defect closure, aortic valve replacement and triple CABG). Another particularity would be the relatively rare etiology (Pneumococcus), but with high severity and mainly encountered in young patients.

In conclusion the complete and accurate preoperative diagnosis in IE and their optimal surgical corrections remain challenging. In the presence of clinical manifestations suggestive for IE, all patients should undergo TTE. In all cases with positive results a TEE is mandatory, in order to identify possible complications for an adequate surgical timing.

References

1. Prendergast BD, Tornos P. Surgery for infective endocarditis: who and when? Circulation 2010; 121: 1141–1152.
2. Habib G, Hoen B, Tornos P, et al. Guidelines on the prevention, diagnosis, and treatment of infective endocarditis (new version 2009): the Task Force on the Prevention, Diagnosis, and Treatment of Infective Endocarditis of the European Society of Cardiology (ESC). Endorsed by the European Society of Clinical Microbiology and Infectious Diseases (ESCMID) and the International Society of Chemotherapy (ISC) for Infection and Cancer. Eur Heart J 2009; 30: 2369–2413.
3. Baddour LM, Wilson WR, Bayer AS, et al. Infective endocarditis: diagnosis, antimicrobial therapy, and management of complications: a statement for healthcare professionals from the Committee on Rheumatic Fever, Endocarditis, and Kawasaki Disease, Council on Cardiovascular Disease in the Young, and the Councils on Clinical Cardiology, Stroke, and Cardiovascular Surgery and Anesthesia, American Heart Association: endorsed by the Infectious Diseases Society of America. Circulation 2005; 111: e394–e434.
4. Hoen B, Duval X. Infective endocarditis. N Engl J Med 2013; 369: 785.
5. Habib G, Lancellotti P, Antunes MJ, et al. 2015 ESC Guidelines for the management of infective endocarditis. The Task Force for the Management of Infective Endocarditis of the European Society of Cardiology (ESC) Endorsed by: European Association for Cardio-Thoracic Surgery (EACTS), the European Association of Nuclear Medicine (EANM)]. Eur Heart J 2015; 36: 3075-3128.
6. Habib G, Badano L, Tribouilloy C, et al. Recommendations for the practice of echocardiography in infective endocarditis. Eur J Echocardiogr 2010; 11: 202–219.
7. Thalme A, Nygren AT, Julander I, Freyschuss U. Classification of infective endocarditis by Duke's criteria and transesophageal echocardiography: a 1-year retrospective analysis. Scand J Infect Dis 1996; 28: 407–410.
8. Strom BL, Abrutyn E, Berlin JA, et al. Risk factors for infective endocarditis: oral hygiene and nondental exposures. Circulation 2000; 102: 2842–2848.
9. Calderwood SB, Swinski LA, Waternaux CM, Karchmer AW, Buckley MJ. Risk factors for the development of prosthetic valve endocarditis. Circulation 1985; 72: 31–37.
10. Mylonakis E, Calderwood SB. Infective endocarditis in adults. N Engl J Med 2001; 345: 1318-1330.
11. Taams MA, Gussenhoven EJ, Bos E, et al. Enhanced morphological diagnosis in infective endocarditis by transoesophageal echocardiography. Br Heart J 1990; 63: 109-113.
12. Flachskampf FA, Wouters PF, Edvardsen T, et al. Recommendations for transoesophageal echocardiography: EAC-VI update 2014. Eur Heart J Cardiovasc Imaging 2014; 15: 353-365.
13. Evangelista A, Gonzalez-Alujas MT. Echocardiography in infective endocarditis. Heart 2004; 90: 614–617.
14. Karalis DG, Bansal RC, Hauck AJ, et al. Transesophageal echocardiographic recognition of subaortic complications in aortic valve endocarditis. Clinical and surgical implications. Circulation 1992; 86: 353-362.

CARDIOVASCULAR FLASHLIGHT
doi:10.1093/eurheartj/ehw407
Online publish-ahead-of-print 22 September 2016

Massive hydropneumopericardium after pericardial drain removal

Ioana Dregoesc[1,2], Adrian Iancu[1,2]*, Adrian Ştef[2], and Adrian Molnar[1,2]

[1]"Iuliu Haţieganu" University of Medicine and Pharmacy, Victor Babeş 8, 400012, Cluj-Napoca, Cluj; and [2]"Niculae Stăncioiu" Heart Institute, Clinicilor 2-4, 400006, Cluj-Napoca, Cluj
* Corresponding author. Tel: +40744751027, Fax: +40264595090, E-mail: adrian_iancu@hotmail.com

A 73-year-old lady was referred to our hospital due to a large pericardial effusion, of unknown origin. Urgent, echo-guided, subxiphoid, percutaneous pericardiocentesis was performed through an 8F-single lumen catheter. The catheter remained in place 24 h and 2700 mL of serohaemorrhagic fluid was drained, with consequent clinical improvement.

The next day following pericardial drain removal, the patient became dyspnoeic. Transthoracic echocardiography revealed swirling echogenic bubbles within the pericardial space (see Supplementary material online, *Panel A*). These findings, consistent with a hydropneumopericardium, were supported by the chest X-ray (*Panel B*), which also raised suspicion of a small left pneumothorax. Computed tomography (CT)

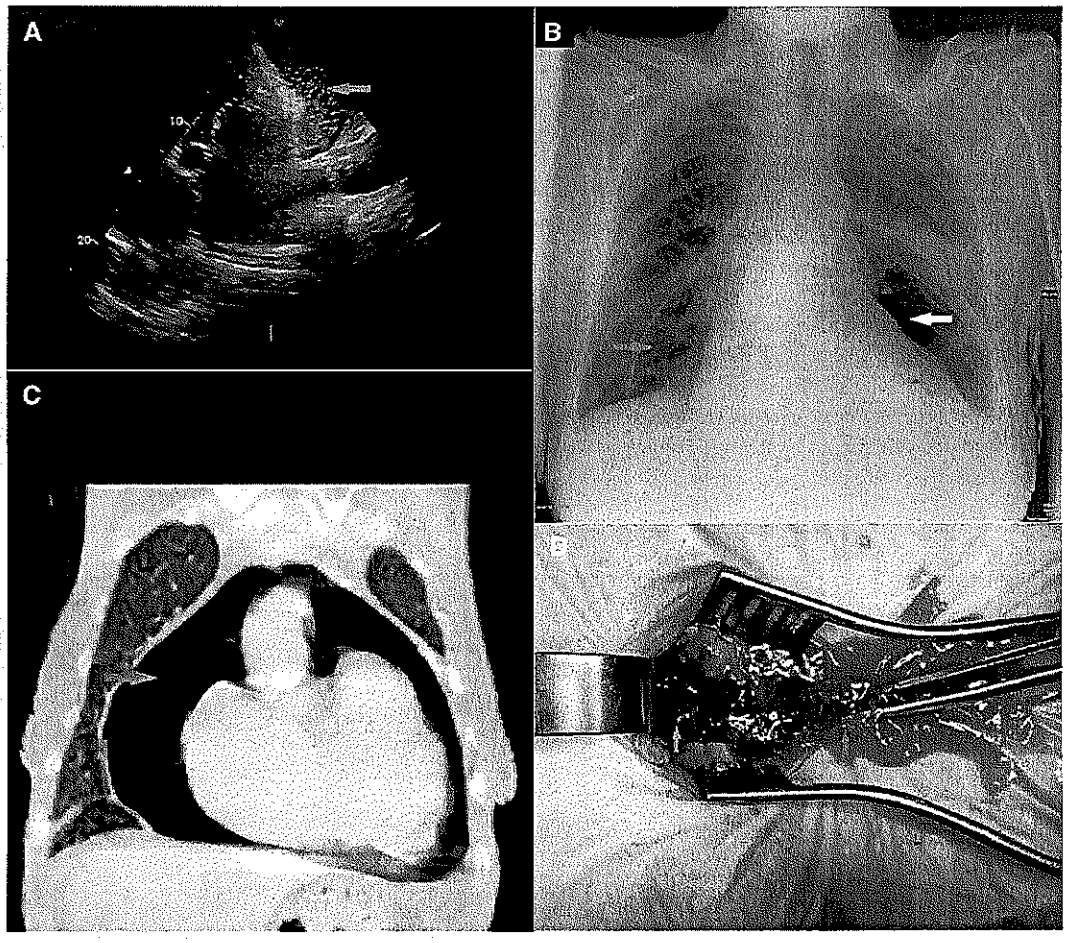

Figure 1 (*Panel A*)—transthoracic echocardiographic modified apical five-chamber view showing echogenic bubbles within the pericardial space (blue arrow) and the persistence of a posterolateral pericardial effusion; (*Panel B*)—chest radiography showing pneumopericardium (blue arrow) and possibly a small left pneumothorax (white arrow); (*Panel C*)—computed tomography frontal view showing massive pneumopericardium (blue arrow); (*Panel D*)—intraoperative image of the pericardial aerated serohaemorrhagic fluid (air bubbles—blue arrow).

confirmed the diagnosis of hydropneumopericardium (*Panel C*). The patient remained hemodynamically stable and therefore we decided for a "watchful waiting" strategy. The control CT performed a week later showed that while the air in the pericardium partially resorbed, the pericardial fluid started to re-accumulate, with an inhomogeneous distribution. Surgical drainage and pericardial biopsy was successfully performed and 1000 mL of aerated serohaemorrhagic fluid was evacuated (*Panel D*). No pleuro-pericardial communication was identified. The histopathologic exam was in favour of a chronic non-specific pericarditis. Besides colchicine therapy, L-thyroxine substitution was initiated for a mild form of hypothyroidism. Given the high prevalence of tuberculosis in the region, the patient was started on tuberculostatic therapy for the 8-week period until the microbiologic laboratory report excluded the diagnosis. Three months later, she was asymptomatic.

We presume that a small pleuro-pericardial communication was produced during pericardiocentesis. The large diameter drain blocked the pleuro-pericardial communication, which opened following catheter removal.

Supplementary material is available at *European Heart Journal* online.

CASE REPORT

RJME
Romanian Journal of Morphology & Embryology
http://www.rjme.ro/

A very rare association between giant right atrial myxoma and patent *foramen ovale*. Extracellular matrix and morphological aspects: a case report

ADRIAN MOLNAR[1)], SVETLANA ENCICĂ[2)], DIANA MARIA SĂCUI[3)], IOAN MUREŞAN[3)], AURELIAN-CĂTĂLIN TRIFAN[3)]

[1)]*"Iuliu Haţieganu" University of Medicine and Pharmacy, Cluj-Napoca, Romania; Clinic of Cardiovascular Surgery, "Niculae Stăncioiu" Heart Institute, Cluj-Napoca, Romania*

[2)]*Department of Pathology, "Niculae Stăncioiu" Heart Institute, Cluj-Napoca, Romania*

[3)]*Clinic of Cardiovascular Surgery, "Niculae Stăncioiu" Heart Institute, Cluj-Napoca, Romania*

Abstract

We report a case of sporadic giant cardiac myxoma with a rare localization in the right atrium, operated in our Service, in a 73-year-old female patient who also presented a patent *foramen ovale* and a history of ischemic stroke in the year prior to current admission. Intra-operatively, the tumor had a very friable, gelatinous aspect, with a high potential for embolization due to its reduced consistency. The present paper refers to clinical, histochemical and immunohistochemical particularities, as well as to macroscopic and microscopic characteristics of the cardiac myxoma, emphasizing the extracellular matrix aspects, and without leaving out the cellular components of this rare tumor, with possible inference in the management of this disease. The authors present their own observations related to the data from the literature. Also, there are some particularities of the case which justify the current presentation.

Keywords: cardiac myxoma, myxoid stroma, extracellular matrix, glycosaminoglycan, hyaluronic acid.

Introduction

Soft tissue tumors are complex mesenchymal lesions with vast differentiation possibilities. In this soft tissue tumors group, the *World Health Organization* (WHO) classification includes benign tumors, malignant tumors, and borderline tumors (locally aggressive but non-metastatic tumors) [1]. In the benign tumors group are comprised the entities with a less known or less understood differentiation course. Being such an entity, cardiac myxoma begins to be outlined like a genetic identity, with obvious chromosomal aberrations [1]. The PRKAR1A gene seems to play a role in the development of the so-called syndromic cardiac myxoma from the Carney complex [2]: it codifies the type I-alpha regulatory subunit of the cAMP-dependent protein-kinase. In the sporadic, common cardiac myxoma, this gene has a less determined role. Now, the literature publishes new data, subsequently to technical progress that allowed the deeper knowledge of these tumors.

Atrial myxoma is the commonest (20–30% of all) primary intra-cardiac tumor in adults and two-thirds of these arise in the left atrium. Other locations are right atrium (next commonest), ventricles, and cardiac valves [3]. Although they are benign, it is recommended their immediate removal as soon as the diagnosis is confirmed, since they are associated with tumor embolization and their harmful consequences [4].

The sufficient and recommended treatment is complete resection of the tumor, associated with the repair of defective area.

Taking into account these considerations, we present the clinical and morphological observations encountered in our case.

Case presentation

A 73-year-old female patient presented in our Service with a four-month history of shortness of breath, accompanied by peripheral edema and palpitations. She also had a history of an ischemic parietal stroke, as well as a radical surgical treatment for duodenal adenocarcinoma in the year prior to her current admission. The cardiovascular, respiratory and abdominal examination was unremarkable and a detailed neurological assessment did not reveal any significant abnormality. The electrocardiogram showed sinus rhythm, with a frequency of 80 bpm (beats per minute), and minor T wave changes in anterior leads.

The trans-esophageal echocardiography (TEE) demonstrated a giant mass (of approximately 65/60/58 mm, with a volume of 63.47 cm^3), which occupies almost entirely the right atrium, prolapsing into the right ventricle, with intermittent obstruction of the tricuspid valve and a very high risk of embolization; the mass was attached to the *ostium secundum* area of the interatrial septum, and also a patent *foramen ovale* with a diameter of approximately 15 mm was present (Figure 1).

The patient accepted the surgical treatment in view of the risks involved, and we performed the complete tumor resection and direct repair (suture) of the atrial septum defect. The surgical approach was made by median sternotomy; we establish the cardio-pulmonary bypass with bi-atrial cannulation, and we tried to avoid tumor

ISSN (print) 1220–0522 ISSN (online) 2066–8279

fragmentation and embolization of its parts. Macroscopically, the excised tumor weighted 55 g, and measured 6.5/6/5.8 cm, with a base of implantation of approximately 1.5/1 cm; its coloration was reddish-blue and yellowish, with a slightly fringed surface, and a gelatinous consistence (Figure 2).

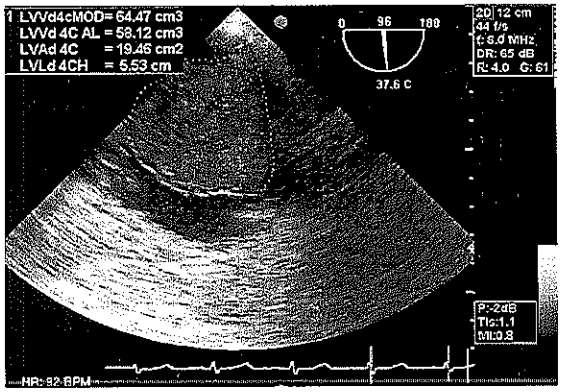

Figure 1 – ***Preoperative image – trans-esophageal echocardiography (TEE): giant mass attached to the ostium secundum area of the inter-atrial septum, occupying almost entirely the right atrium and prolapsing into the right ventricle, with intermittent obstruction of the tricuspid valve.***

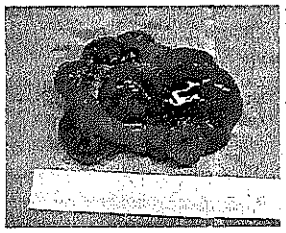

Figure 2 – ***Tumor aspect after surgical removal: gelatinous consistence with a slightly fringed surface, reddish-blue and yellowish coloration, measuring 6.5/6/5.8 cm, with a base of implantation of approximately 1.5/1 cm (arrow).***

We studied multiple fragments from the atrial mass, embedded in paraffin by the routine method; the slices were examined with an Axioskop 40 microscope (Carl Zeiss). The sections were taken at 5 μm, and stained with Hematoxylin–Eosin (HE); we also practiced histochemical and immunohistochemical stains; histochemical stains were Orcein, Masson's trichrome, Alcian blue, Periodic Acid–Schiff (PAS) and Mucicarmine, in order to stand out the particularities of the tumoral matrix. The immunomarking was achieved following multiple steps, one of them being the thermal processing of sections (in a period of 15 minutes, in citrate buffer with a pH of 6). The primary antibodies were applied in the following dilutions: calretinin – 1:100, vimentin, clone 9 – 1:100, desmin – 2:100, Ki67 – 1:100, S100 – 1:4500, CD31 – 5:100. The technique followed the steps of the Streptavidin–Biotin system (the LSAB universal kit), and the chromogenic base for peroxidase was 3,3'-Diaminobenzidine (DAB). For this reason, the positive cells are brownish; the counterstaining was made with watery Hematoxylin, determining the bluish tint of the background.

Microscopically, the multiple tumor fragments analysis showed the presence of a myxoid stroma containing polygonal or stellate cells with eosinophilic cytoplasm and oval nuclei with possible visible nucleolus. The myxoma cells were disposed in a perivascular, annular design, and arranged in groups and strings (Figure 3).

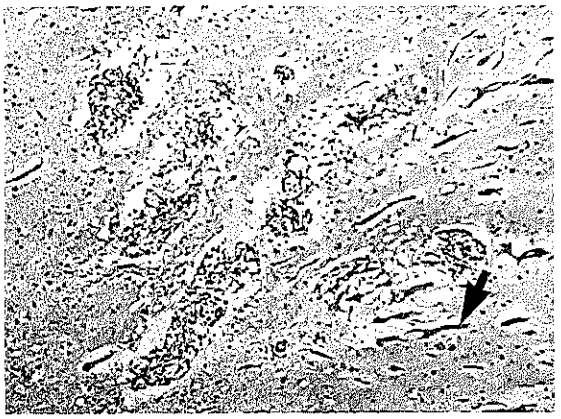

Figure 3 – ***Microscopic aspect of the cardiac myxoma (HE staining, ×100): the cells are arranged in perivascular rings (green arrow), and embedded in a myxoid stroma, some of them being arranged in groups and strings (black arrow).***

The lepidic cells are positive for calretinin, S100, and CD31. By the CD31 antibody, there is evidence of endothelial cells in the vascular structures, surrounded by the mentioned annular structures formed by the myxoma cells (Figure 4).

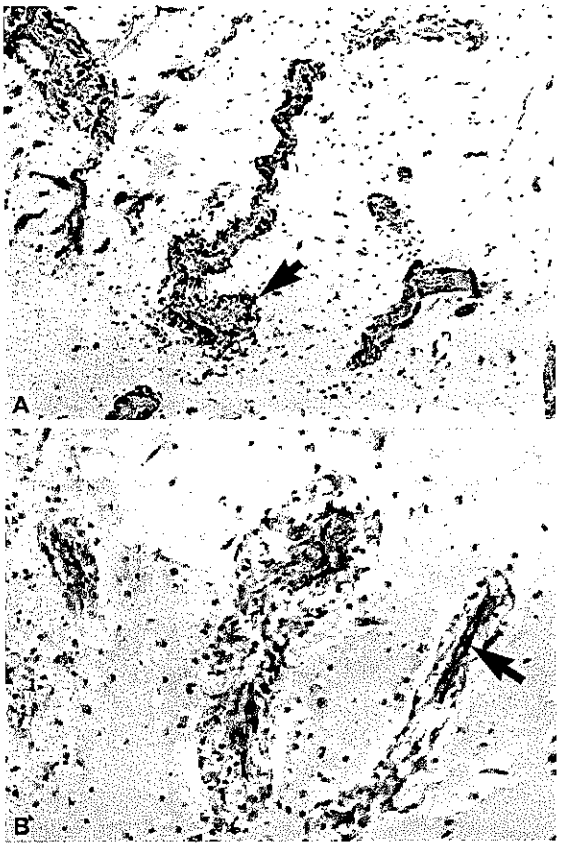

Figure 4 – ***Immunohistochemical stainings for calretinin (A) and CD31 (B). The myxoma cells are positive for calretinin (A): green arrow for groups of lepidic cells and black arrow for rings; the endothelial cells positive for CD31 (B) (black arrow) delineate the vascular channels surrounded by the annular structures composed by myxoma cells.***

The tumoral stroma contains elastic fibers (Figure 5) and is constituted of mucin areas, revealed by Mucicarmine and PAS stainings (Figure 6).

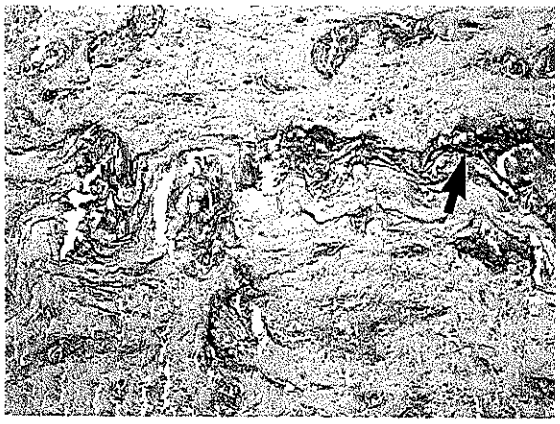

Figure 5 – *The Orcein staining (×100) reveals the presence of elastic fibers in the myxoma matrix (arrow).*

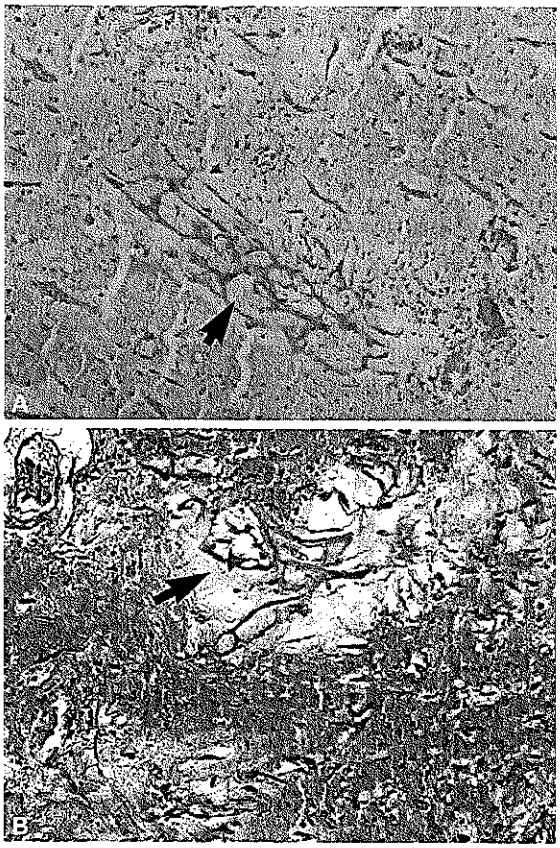

Figure 6 – *(A) Mucicarmine staining (×100) reveals the central points that contain mucins in the extracellular matrix. (B) PAS staining (×100) performed with the same purpose (arrows).*

Also, the myxoid stroma in our case is very rich in proteoglycans, shown by the Alcian blue staining (Figure 7). Beyond these stromal components, we also identified the presence of lymphocytes and macrophages. The histological exam of the implantation base revealed the complete excision of the myxoma. The Ki67 proliferation factor was less than 5% of the studied material.

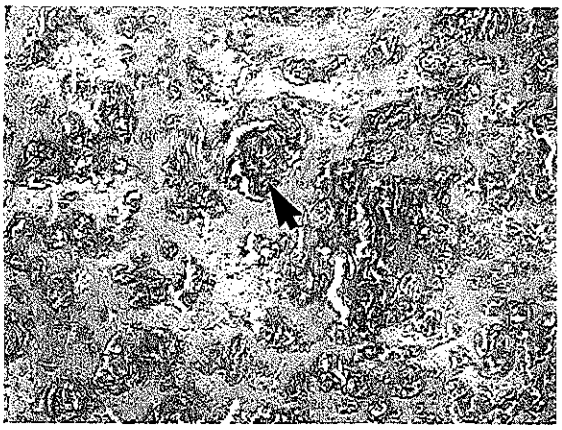

Figure 7 – *Alcian blue staining (×200) reveals the rich component of proteoglycans in the myxoid tumoral stroma (arrow).*

Discussion

The first mention of a cardiac tumor was made by Realdo Colombo in 1559, but only in 1952 the first antemortem study of an atrial myxoma was published.

The first successful myxoma resection was accomplished in 1954. Based on autopsy findings, the incidence of primary cardiac tumors vary between 0.0017% and 0.25%. Of all primary cardiac tumors, 3/4 are benign and 1/4 are malignant. Of the benign tumors, myxoma is by far the most common, reaching an incidence of about 50%. Regarding the localization, the most frequent is in the left atrium (over 75% of cases), then in the right atrium (15–20% of cases), and the rest could be found in the left ventricle, right ventricle and bi-atrial [5].

In our clinic experience, of 84 cases of myxoma operated between 1991 and 2014, only in 12 cases the myxoma was situated in the right atrium, and only in the presented case the tumor was accompanied by a patent *foramen ovale*.

The term "myxoma" was first introduced by Rudolf Virchow in order to describe the soft tissue tumors structurally resembling the umbilical cord. He used in 1863 the term of myxoma to delineate the tumors he has already described in 1861, as having macroscopic and microscopic characteristics similar to Wharton's gelatin from the umbilical cord [6]. Also, Rudolf Virchow introduced this term as a pathologic entity [7]. The "Medical Lexicon" by Robley Dunglison specifies that the "myxoma" term was first presented by Johannes Müller under the name of "collonema". The term designated a gelatinous tumor, which trembled when being touched [8]. Myxoid tumors are presently classified according to complex clinical and pathologic criteria, and to molecular and cytogenetic characteristics [7].

Presently, there are three theories that explain the myxoma cells' histogenesis: the thrombogenic theory, the neoplasic theory, and the hamartoma theory.

Cardiac myxoma contains a great variety of cells that are believed to originate in the mesenchymal pluripotent stem cells in the *fossa ovalis*, known as Prichard's structures [2]. The myxoma cells, known as lepidic cells, produce the extracellular matrix of the tumor. They are

revealed by the expression of calretinin, as we could see in our case. Calretinin is intensely expressed in the cytoplasm and nucleus of cardiac myxomas, this antibody being proposed as immunohistochemical marker of this tumor since 2003 [9–11]. The lepidic cells can express S100, actin, CD31 and vimentin. Variably, it was demonstrated that there could also be found other positive markers like CD34, myoglobin, desmin, factor VIII, which could be used for explaining the origin of the tumor from mesenchymal pluripotent cells with variable differentiation potential [12–15]. Other cells are represented by lymphocytes, siderophages, plasmacytes, and histiocytes. The blood vessels are numerous and rudimentary, paved by CD31-positive endothelial cells [2]; this aspect is shown in Figure 4B, proving the cellular components of the above-described myxoma.

The histological features necessary for the diagnosis of myxoma are the identification of lepidic cells, surrounded by a gelatinous environment, with rudimentary vascular channels and macrophages with hemosiderin.

The cells are embedded in a gelatinous environment, determining tumor friability, which can embolize spontaneously or during surgical intervention.

Tumor fragment embolization can be produced at any vascular level. The tumor cells are viable and remain attached to the vascular wall [16, 17].

There were some reports on cases with myxoma emboli at pulmonary or cerebral level; the embolized myxoma cells had the ability of multiplying inside the arterial wall where they were quartered, and determining fusiform aneurysm formation.

Cardiac myxoma is not considered a malignant tumor. The myxoma malignancy is determined by its behavior, and not by its histological aspect. Cardiac myxomas were regarded as mild proliferative lesions, with low metastatic potential, and without modulation of oncogenes or tumoral suppressing genes [18].

The lepidic cells produce the myxoid stroma, in which they are embedded, and consequently we granted special attention for this tumoral component.

The extracellular matrix composition was better assessed after introducing the Alcian blue staining in 1950 [7], which identify the presence of glycosaminoglycans in the tissue sections.

The glycosaminoglycans are macromolecules found in the pericellular space and in the extracellular matrix: hyaluronic acid, keratan sulfate, chondroitin sulfate, dermatan sulfate, heparin sulfate, and heparin. The glycosaminoglycans form proteoglycans by specific connections with proteic cores. The proteoglycans are grouped in three families: the lecticans, the small proteoglycans enriched with leukines and the extracellular matrix proteoglycans.

The glycosaminoglycans have specific biophysical characteristics like high viscosity and reduced compressibility. Their rigidity implicates them in maintaining the tissular integrity, by favoring the cellular diffusion and migration. The biochemical characteristics of glycosaminoglycans are mediated by specific connections with other macromolecules in the extracellular matrix.

Besides glycosaminoglycans, the extracellular matrix contains collagen and other molecules as fibronectin and tenascin. In the soft tissue tumors like myxoma, the extracellular matrix is heterogeneous. The cardiac myxoma contains chondroitin-4-sulfate (C4S), chondroitin-6-sulfate (C6S), and hyaluronic acid (HA). The HA seems to be the major component in determining the myxoid aspect of the extracellular matrix [7].

C4S and C6S are glycosaminoglycans that enter in the composition of skin, cartilages and tendons, and play a physiological role in ionic bonding (calcium, copper and iron ions), with anti-oxidative effects and reducing the apoptosis and pro-inflammatory cytokines [7].

By biochemical methods, it was proved that the HA content of cardiac myxoma is 30-times higher than in the normal interatrial septum [19]. The HA is present in the heart during its development and it participates to tissular remodeling, regeneration and reparation processes, embryogenesis, and carcinogenesis [7, 19]. The HA is also abundant in the bones and cartilages. It is involved in early tissular organization by facilitating the migration and condensation of mesenchymal cells; it intervenes in the articular cavity formation, the osteoclastic and osteoblastic functions. It favors the reduction of pain perception and has a suppressing effect on cartilage degeneration [7].

Conclusions

The association between a right atrial myxoma and a patent *foramen ovale* is extremely rare, being mentioned in only six case reports from the English specialized literature. This association, along with the history of an ischemic stroke, the giant tumor size, and the patient's advanced age (knowing the fact that cardiac myxoma usually affects younger patients – less than 50-year-old), constitute particularities that determined us to present and discuss this case. In the mean time, we analyzed the extracellular matrix components in order to understand the causes of its friability and its particular behavior. We consider that cardiac myxoma is a tumor with origin in the pluripotent mesenchymal cells, with differentiation capacity from multiple cell lines. We believe that supplementary studies on the constitutive elements of this rare tumor could bring useful information about the tumor's recurrence mechanisms and behavior, with possible therapeutic consequences.

Conflict of interests

The authors declare that they have no conflict of interests.

References

[1] Dei Tos AP, Dal Cin P. The role of cytogenetics in the classification of soft tissue tumours. Virchows Arch, 1997, 431(2):83–94.
[2] Maleszewski JJ, Burke AP. Cardiac myxoma pathology. Medscape, http://emedicine.medscape.com/article/1612513-overview, Updated: February 2, 2014.
[3] Biswas A, Thakur AK. An unusual presentation of atrial myxoma in an elderly patient: a case report. Cases J, 2008, 1(1):384.
[4] Lorentz MN, Vrandecic EC, Drumond LF, Soares RR. Right atrial myxoma associated with acute cor pulmonale. Case report. Rev Bras Anestesiol, 2008, 58(1):69–72.
[5] Bethea BT, Richter A. Chapter 48: Primary cardiac tumors. In: Yuh DD, Vricella LA, Yang S, Doty JR (eds). Johns Hopkins textbook of cardiothoracic surgery. 2nd edition, McGraw–Hill Education, 2014, 753–767.

[6] Glicenstein J, Ohana J, Leclercq C. Myxoma. In: Glicenstein J, Ohana J, Leclercq C. Tumours of the hand. Springer-Verlag, Berlin–Heidelberg–New York–London–Paris–Tokyo, 1988, 85–88.
[7] Willems SM, Wiweger M, van Rogen JFG, Hojendonn PCW. Running GAGs: myxoid matrix in tumor pathology revisited: what's in it for the pathologist? Virchows Arch, 2010, 456(2): 181–192.
[8] Dunglison R. Medical Lexicon: a dictionary of medical science. 13th edition, revised. Blanchard and Lea, Philadelphia, 1856, 221.
[9] Chopra P, Ray R, Singh MK, Venugopal P. Cardiac myxoma with glandular elements: a histologic, histochemical and immunohistochemical evaluation. Indian Heart J, 2003, 55(2): 182–184.
[10] Acebo E, Val-Bernal JF, Gómez-Roman JJ. Thrombomodulin, calretinin and c-kit (CD117) expression in cardiac myxoma. Histol Histopathol, 2001, 16(4):1031–1036.
[11] Acebo E, Val-Bernal JF, Gómez-Román JJ. Prichard's structures of the fossa ovalis are not histogenetically related to cardiac myxoma. Histopathology, 2001, 39(5):529–535.
[12] Burke A, Virmani R. Tumors of the heart and great vessels. Atlas of tumor pathology. 3rd Series, Fascicle 16, Armed Forces Institute of Pathology (AFIP), Washington, DC, 1996, 21–47.
[13] Hudson REB. Cardiovascular pathology. Edward Arnold Ltd., London, 1965, 1563–1603.
[14] Becker AE. Tumors of the heart and pericardium. In: Fletcher CDM (ed). Diagnostic histopathology of tumors. Churchill–Livingstone, New York, 1995, 7–38.
[15] McMannus B. Heart disease in the adult. In: Damjanov I, Linder J (eds). Anderson's pathology. 10th edition, Mosby–Year Book, St. Louis, 1996, 1309–1338.
[16] Kanda T, Sakamaki M, Murata K. A cardiac myxoma with interleukin-6 production and cerebral metastasis. Int J Cardiol, 1994, 45(2):144–146.
[17] Alkhulaifi AM, Homer S, Pugsley WB, Sturridge MF. Recurrent left atrial myxoma. Cardiovasc Surg, 1994, 2(2):232–236.
[18] Bârsan M, Encică S, Scridon T, Şerban A, Manole S, Andrieş G (red). Clasificarea histologică a tumorilor cardiace. Histogeneza tumorilor cardiace. Ed. Medicală Universitară "Iuliu Haţieganu", Cluj-Napoca, 2007, 20–36, 66–84.
[19] Longaker MT, Chiu ES, Hendin B, Finkbeiner WE, Stern R. Hyaluronic acid in a cardiac myxoma: a biochemical and histological analysis. Virchows Arch A Pathol Anat Histopathol, 1991, 418(5):435–437.

Corresponding author
Adrian Molnar, Assistant Professor, MD, PhD, "Iuliu Haţieganu" University of Medicine and Pharmacy, Cluj-Napoca; Clinic of Cardiovascular Surgery, "Niculae Stăncioiu" Heart Institute, 19–21 Moţilor Street, 400001 Cluj-Napoca, Romania; Phone +40264–591 941 int. 220, e-mail: adimolnar45@yahoo.com

Received: January 8, 2016

Accepted: May 17, 2016

Giant Infrarenal Aortic Aneurysm Rupture Preceded by Left Lower Limb Motor Deficit

Sasarman Vasile Aurelian,[1,2,4] Molnar Adrian,[2,4] Bindea Dan,[2,4] Schjoth Bruno,[1,4] Oprea Alexandru,[2,4] Trifan Catalin,[2,4] and Andercou Octavian,[3,4] Metz, France and Cluj-Napoca, Roumania

This report presents the surgical repair and postsurgical outcomes following a ruptured infrarenal aortic aneurysm with a maximum transverse diameter of 20 cm. Its association with acute lower limb motor deficit is rare. Open surgery of giant abdominal aortic aneurysms is often the only available treatment, favored over an endovascular approach in the presence of increased aneurysm size with dislodged abdominal organs, adhesions, and short and angled proximal infrarenal aortic neck, presenting significant additional surgical and anesthesiological challenges.

CASE REPORT

A 64-year old male with a medical history of hypothyroidism, acute pancreatitis (for which he underwent surgery in 2012), and hypertension was brought to the Emergency Department presenting syncope. The patient also complained of back pain and left lower limb motor deficit, which had been present for about 2 weeks without sensory deficit. The lower limbs had no signs of ischemia, and the femoral pulse was bilaterally palpable. Furthermore, for the month prior to presentation, the patient suffered alternating bouts of diarrhea and constipation. Upon admission, the patient was malnourished. His body mass index was 19, blood pressure was 80/60 mm Hg, heart rate was 100 bpm, and clinical status was otherwise normal. Physical examination revealed a pulsatile, well-defined, voluminous abdominal mass stretching from the inferior margin of the left costal margin to the left superior iliac crest, exceeding the midline.

Blood tests revealed hemoglobin was 4.8 g/dL, hematocrit was 16%, plasma creatinine was 24 mg/L, urea was 2.37 g/L, leukocyte count was 16,000 U/μL, erythrocyte sedimentation rate was 80 mm/hr, and C-reactive protein was 242 mg/L. The elevated creatinine level warranted an abdominal computed tomography (CT) scan without contrast, which revealed a large infrarenal abdominal aortic aneurysm (AAA) with a transverse maximum diameter of 19.8 cm and signs of posterior rupture (Fig. 1).

The mass occupied a large amount of the volume in the abdominal cavity, causing severe compression of the left kidney; spleen; and transverse, left, and sigmoid colon (Fig. 2). The CT revealed that about 1 cm of the proximal part of the aorta beneath the right renal artery was undilated, while the left renal artery was not visible and the proximal infrarenal aortic neck was angled at 130°. Because of the extreme dimensions of the aneurysm, the angulation of the aorta, sinuous trajectories of the iliac arteries, and the clinical status of the patient, the endovascular approach was considered inadequate in favor of open surgery.

An emergent open transperitoneal repair was performed using a Y-shaped Dacron graft (16 × 8 mm). In the presence of dense adherences of structures adjacent to the aneurysm wall and the large size of the aneurysm, isolation and aortic cross-clamping of the proximal infrarenal aortic neck was performed with difficulty. Aortotomy was executed along the anterior wall of the aneurysm, and a large intraluminal thrombus mass was extracted. Proximal anastomosis with the infrarenal aorta was performed just below the renal arteries, whereas distal anastomoses involved the right and the left common femoral arteries. A decision was made not to reimplant the inferior mesenteric artery because it was overly thrombotic. During the procedure, high doses of inotropes were required. The patient also received 9 units of red blood cells, 6 units of frozen plasma, 1 unit of cryoprecipitate, and 3 grams of human fibrinogen.

[1]*Regional Hospital Center Metz-Thionville, Hôpital de Mercy, Metz, France.*

[2]*Heart Institute "Niculae Stancioiu" Cluj-Napoca, Cluj-Napoca, Roumania.*

[3]*Vacular Surgery Clinic, Cluj-Napoca, Roumania.*

[4]*University of Medicine and Pharmacy Iuliu-Hatieganu, Cluj-Napoca*

Correspondence to: Molnar Adrian, Street Rosetti, nr 7, ap 2A, Cluj-Napoca, Roumanie 400306; E-mail: sasa_umf@yahoo.com

Ann Vasc Surg 2017; 43: 317.e13–317.e16
http://dx.doi.org/10.1016/j.avsg.2017.03.182

Manuscript received: September 29, 2016; manuscript accepted: March 5, 2017; published online: 4 May 2017

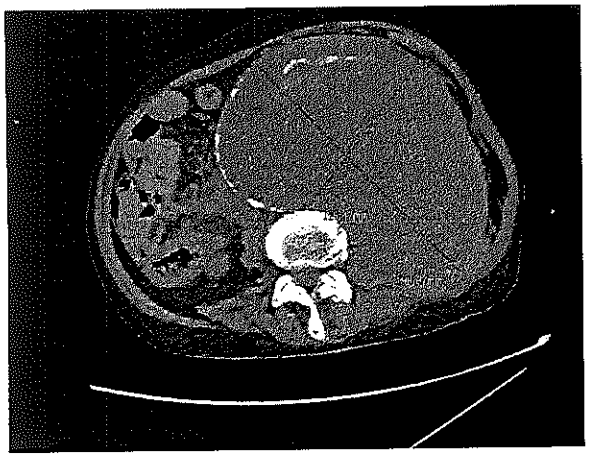

Fig. 1. Abdominal CT showing a large infrarenal abdominal aortic aneurysm with a transverse maximum diameter of 19.8 cm.

Postsurgical evolution of the patient was marked by the possibility of rapid reduction of inotropic support with hemodynamic stability and preserved diuresis. Severe thrombocytopenia was developed and corrected through further transfusion of blood derivatives (negative platelet aggregation and heparin-PF4 antibody tests). At the fourth postoperative day, as a result of repeated episodes of diarrhea, a colonoscopy was performed, revealing moderate ischemic colitis. An abdominal contrast CT was performed on the 10th postoperative day, showing a lack of perfusion in the posterior part of the left kidney (thrombosed left renal artery), while the organ was otherwise vascularized by a patent accessory renal artery (Fig. 3).

In addition, a small retroperitoneal effusion was revealed. Other radiologic findings were normal, and the Dacron graft showed good blood flow. The left lower limb showed no postprocedural amelioration of the motor deficit.

Histological examination of the dilated aortic wall revealed a thick layer of adherent intraluminal thrombus overlying an atheromatous intima. Mucoid extracellular matrix accumulation with the presence of sporadic cholesterol crystals resulted in separation of the intima with visible inflammatory infiltration, numerous dystrophic points of calcification, and subsequent medial atrophy. The adventitia was abundant with lymphocytes, thickened from inflammation. Four hyperplastic ganglions were isolated from the periaortic adipose tissue.

DISCUSSION

Ischemic colitis following aortic surgery is a serious complication. Its incidence varies from 0.6% to 3% in nonruptured AAA repairs to 7% to 27% in ruptured AAA repairs.[1] The incidence rate is influenced by the surgical technique employed; the frequency is 22% when aortofemoral grafts are used, 4% when tube grafts are used, and 2.7% when aortoiliac grafts are used.[2] Preoperative shock is the most important factor predicting the development of colon ischemia following AAA rupture. Other risk factors are elevated intraabdominal pressure, renal failure requiring dialysis, use of vasopressors and intraoperative transfusions, IMA patency, collateral supply from the superior mesenteric artery, and internal iliac artery.

We chose not to reimplant the IMA on the basis of its intraoperative aspect (thin vessel, thrombosed) even though preoperative angiographic assessment of the colon blood supply was not available. Our decision was further supported by the nonischemic macroscopic aspect of the sigmoid colon after aortic declamping. Objective means of assessing collateral circulation other than IMA back-bleeding or use of a macroscopic aspect of the colon are: colon mucosal saturation measurement, laser Doppler flowmetry, IMA stump pressure measurements, and use of a photoplethysmographic technique.

Rectosigmoidoscopy, which is the diagnostic procedure of choice, should be systematically performed after AAA rupture, allowing for detection of colon ischemia at an earlier stage.[3]

We could not identify the left renal artery on the native CT scan before surgery primarily because of the largeness of the aortic aneurysm; however, during the procedure, we were able to find and isolate the initial part of the vessel. The artery was ectatic and had a trajectory that was initially sinuous but became severely angulated by the aneurysm, which also compressed the left kidney. Even though a renal artery occlusion can occur as a complication of aortic surgery, we presumed that in this case, it was closely correlated with the morphology of the vessel and its position relative to the aneurysm: the obstruction was favored by its dilation, tortuosity, and angulation.

Aneurysm size is the most important factor related to likelihood of rupture; the risk increases substantially when the aneurysm is large. The annual rupture rate is 30—50% when the AAA is more than 8 cm in diameter.[4] Associated acute lower limb motor deficit is rare. Repairing large aortic aneurysms presents a significant additional surgical and anesthetic challenge because of a variety of factors: its size, which can result in displacement of abdominal organs; the presence of adhesions, which may increase the rupture rate; short and angled proximal infrarenal aortic neck; and sinuous trajectories of the iliac arteries. Further difficulties may arise if a giant aneurysm ruptures, leading to massive bleeding, adjacent hematoma, coagulopathy, and, ultimately, shock. Other documented risk factors for negative

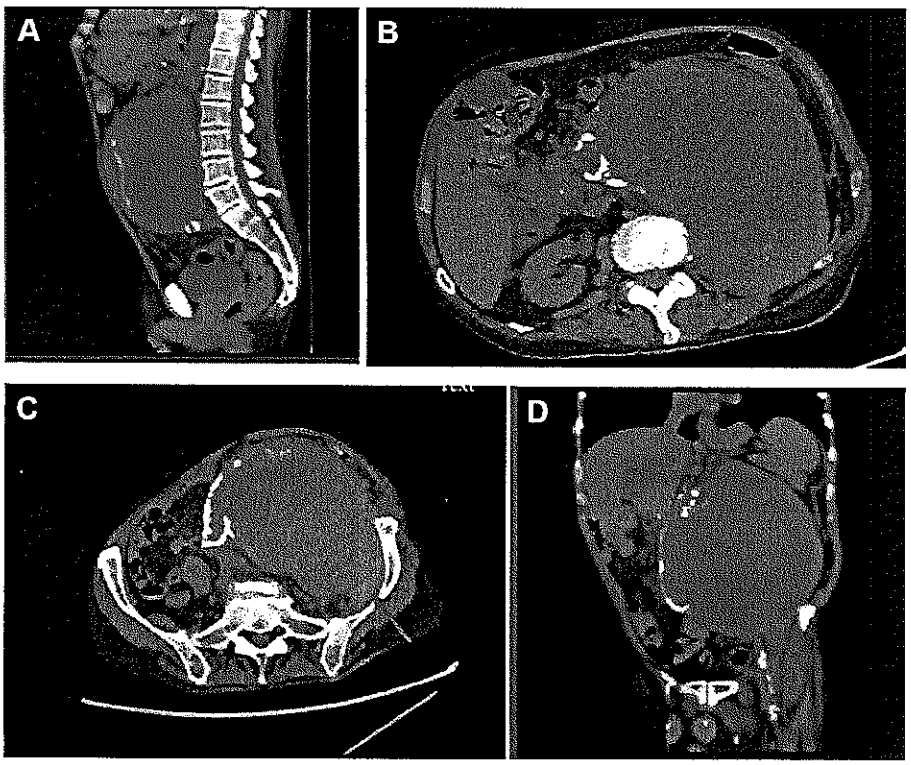

Fig. 2. Abdominal CT showing: **(A)** and **(B)** giant abdominal aortic aneurysm compressing the intraabdominal organs; **(C)** and **(B)** a large hematoma (*arrow*) and signs of posterior rupture.

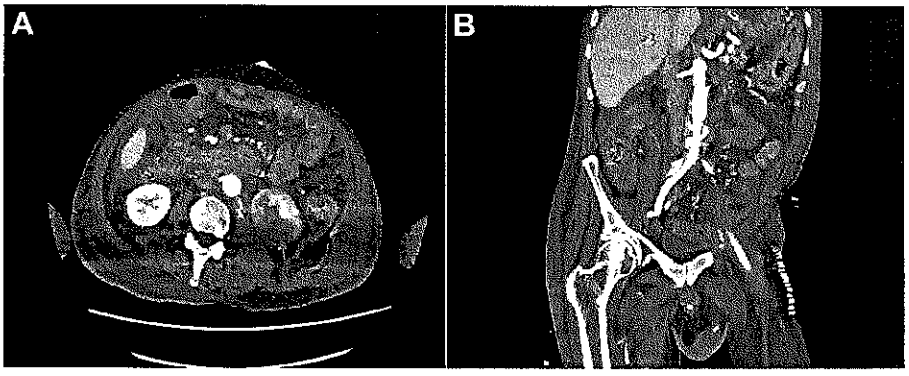

Fig. 3. Postoperative CTA showing: **(A)** lack of perfusion of the posterior part of the left kidney (*arrow*); **(B)** aortic graft with normal flow.

outcomes include the following: age, coronary artery disease, inferior mesenteric artery patency, need for vasopressor use, and intraoperative transfusions. Endovascular repair is frequently not suitable for giant AAAs because of anatomic limitations.[5]

To avoid complications, we recommend that the internal iliac artery (particularly on the left side) and mesenteric collateral vessels (Arc of Riolan) be preserved, the IMA be reimplanted, and periprocedural hypotension be avoided. Vural et al.[6] suggest hypothermic total circulatory arrest, and open

proximal anastomosis techniques may be helpful in giant AAA repair.

Unfortunately, the evolution was unfavorable. In the third week postintervention, the patient developed acute respiratory distress syndrome as a result of aspiration pneumonia, which evolved into septic shock and exitus.

REFERENCES

1. Levison JA, Halpern VJ, Kline RG, et al. Perioperative predictors of colonic ischemia after ruptured abdominal aortic aneurysm. J Vasc Surg 1999;29:40–5.
2. Becquemin JP, Majewski M, Fermani N, et al. Colon ischemia following abdominal aortic aneurysm repair in the era of endovascular abdominal aortic repair. J Vasc Surg 2008;47: 258–63.
3. Biros E, Staffa R. Incidence and risk factors of ischemic colitis after AAA repair in our cohort of patients from 2005 through 2009. Rozhl Chir 2011;90:682–7.
4. Brewster DC, Cronenwett JL, Hallett JW Jr, et al. Guidelines for the treatment of abdominal aortic aneurysms. Report of a subcommittee of the Joint Council of the American Association for Vascular Surgery and Society for Vascular Surgery. J Vasc Surg 2003;37:1106–17.
5. Choi JY, Burton P, Walker S, et al. Abdominal compartment syndrome after ruptured abdominal aortic aneurysm. ANZ J Surg 2008;78:648–53.
6. Vural H, Türk T, Göncü T, et al. Giant size abdominal aortic aneurysm repair using open proximal anastomosis un- der hypothermic circulatory arrest: a report of two cases. J Vasc Surg 2007;46:363–5.

Case report

Med Ultrason 2019, Vol. 21, no. 2, 194-196
DOI: 10.11152/mu-1741

The role of echocardiography in the diagnosis and management of a giant unruptured sinus of Valsalva aneurysm

Adela Şerban[1,2], Nicoleta Bătrâna[1], Mihai Cocoi[1], Raluca Ianoş[1], Ştefan Moţ[1], Emese Kovacs[1], Dan Damian Axente[2,3], Carmen Man[4], Adrian Molnar[2,5]

[1]Cardiology Department, "N. Stancioiu" Heart Institute, [2]"Iuliu Haţieganu" University of Medicine and Pharmacy, [3]5th Surgical Department, Municipal Clinical Hospital, [4]Military Hospital, [5]Cardiovascular Surgery Department, "N. Stancioiu" Heart Institute, Cluj-Napoca, Romania

Abstract

Sinus of Valsalva Aneurysm (SVA) is an aortic root anomaly, consisting of a lack of continuity between the aortic media and the aortic annulus, caused by a structural deficiency of muscular and elastic tissue. We present the case of a 49-year-old man with atypical chest pain. Echocardiographic imaging described a giant unruptured aneurysm of the right sinus of Valsalva which was confirmed by cardiac computed tomography and coronary angiography. The obstruction of the right coronary artery without intravascular thrombosis and the compression of the right ventricular outflow tract with dynamic obstruction gradient represent the particularities of our case.

Keywords: sinus of Valsalva; aneurysm; aorta

Introduction

Sinus of Valsalva aneurysm (SVA) is defined as a significant enlargement of one or more of the aortic sinuses located between the aortic valve annulus and the sinotubular junction. The estimated incidence is approximately 0.09% in general population. Congenital aneurysms are more prevalent than acquired ones [1]. Usually the right coronary sinus is affected (70-90%). Unruptured SVA is often asymptomatic but occasionally can cause severe complications due either to the compression of adjacent cardiac structures or to its rupture [1,2].

Transthoracic echocardiography (TTE) is the modality of choice for SVA screening, with a high sensitivity and more than 90% diagnostic accuracy. Transesophageal echocardiography (TEE) due to its better acoustic window is strongly recommended and can improve the image quality, revealing fine structures (e.g. thrombus, vegetations, small aneurysmal defects) [2].

Received 03.10.2018 Accepted 22.11.2018
Med Ultrason
2019, Vol. 21, No 2, 194-196
Corresponding author: Şerban Adela Mihaela MD, PhD
Cardiology Department, Heart Institute
19-21, Motilor street,
400001, Cluj-Napoca, Romania
Phone: +40-264-591.941
E-mail: adelamserban@yahoo.com

Case report

A 49-year-old man was admitted with atypical chest pain unrelated to physical activity and radiating into the right shoulder. There was no history of fever, collagen or vascular diseases. The physical examination was unremarkable. Electrocardiogram showed no signs of ischaemia and the chest radiography described cardiomegaly with right atrium enlargement.

Routine TTE, performed with a GE Vivid S6 echo system using a 1.5-3.6 MHz probe, discovered severe aortic root dilatation at the level of the sinus of Valsalva with a large saccular structure arising from the right sinus; the aortic valve was tricuspid with trivial aortic regurgitation, ascending and descending aorta were within normal limits (fig 1a,b). The colour Doppler mode detected turbulence in the right ventricular outflow tract (RVOT) with a dynamic gradient of 23 mmHg and a peak velocity of 2.5 m/s measured by continuous wave Doppler mode.

A TEE was performed (GE Vivid 6 echo system, 2.9-8 MHz probe). The bi-dimensional images at mid-esoph-

ageal level confirmed the presence of a right coronary sinus aneurysm, with maximum dimensions of 53x51 mm, with intrasaccular vortex, with layered thrombus along its walls. We followed the continuity of the SVAs walls and no sites of rupture were detected. The aneurysm was protruding into the right ventricle, with distortion of RVOT. Congenital defects such as ventricular septal defects, aortic regurgitation and bicuspid aortic valve were excluded (fig 1c,d).

For precisely delineating the anatomic relationships of the aneurysm and for evaluation of the coronary anatomy, a contrast enhanced cardiac computed tomography (CT) was performed. The aneurysm was not homogeneously opacified by the contrast and was protruding into the right cavities (fig 2). The right coronary artery (RCA) was described as thin, filiform.

Coronary angiography was considered necessary to distinguish the sinus aneurysm from other coronary

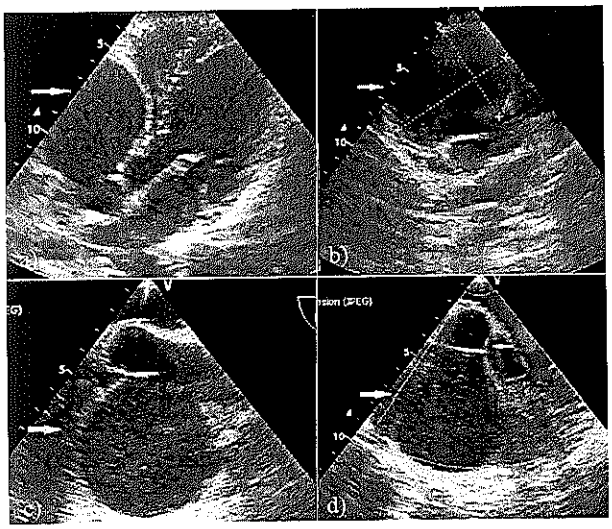

Fig 1. Transthoracic echocardiography: a) apical 5-chambers view: right sinus Valsalva aneurysm (arrow); b) parasternal short axis view at great vesssels level: aneurysm measuring 55x70 mm. Transesophageal echocardiography – mid-esophageal level: c) long axis view of the aortic valve and ascending aorta: large right sinus of Valsalva aneurysm (arrow), with vortex; d) short axis view of the aortic valve, colour Doppler: aneurysm of the right sinus Valsalva (yellow arrow) and a tricuspid aortic valve (white arrow).

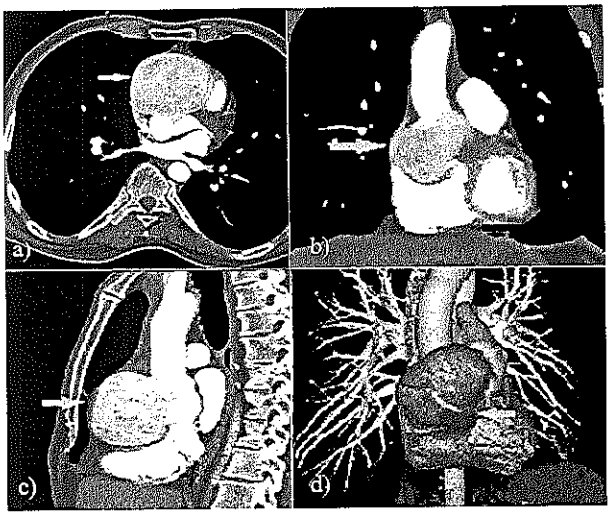

Fig 2. Contrast-enhanced cardiac computed tomography and 3D reconstruction: a) axial, b) coronal and c) sagittal reconstructed images: right sinus of Valsalva aneurysm (arrow) with nonhomogeneous opacification of the contrast; d) 3D reconstructed CT angiography: giant aneurysm of sinus Valsalva is clearly seen (arrow).

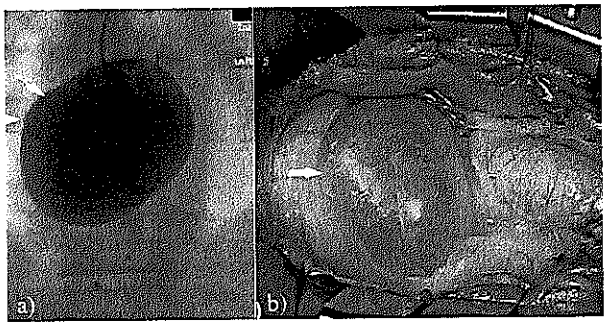

Fig 3. Aneurysm of the right sinus of Valsalva (arrows): a) coronary angiography; b) intraoperative image

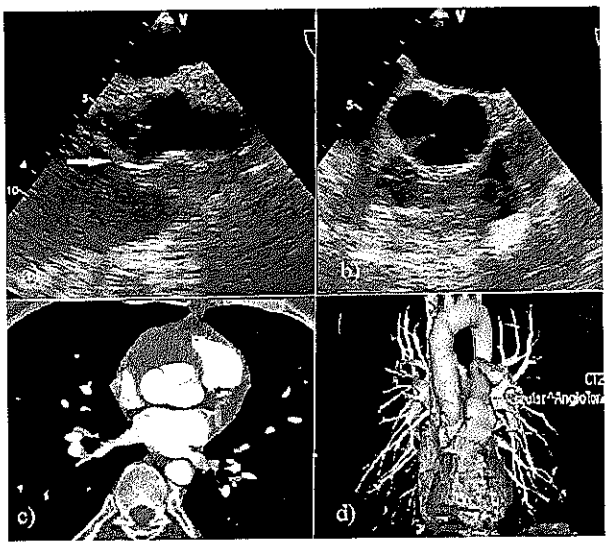

Fig 4. Postoperative images. Transesophageal echocardiography: a) mid-esophageal level, long axis view of the aortic valve and ascending aorta: aortic root with neosinus reconstruction (arrow); b) mid-esophageal level, short axis view of the aortic valve: normal aortic valve; c) and d) contrast-enhanced cardiac computed tomography and 3D reconstruction: tubular Dacron prosthesis between the aortic root and ascending aorta.

anomalies (e.g. a coronary aneurysm). A nonselective injection in the right sinus showed absence of flow in the RCA. The selective injection in the left main showed normal left anterior descendant and normal left circumflex coronary artery with well developed collaterals completely filling the right coronary artery until its proximal segment (fig 3a).

The patient was referred for cardiac surgery. An aneurysmectomy with interposition of a tubular Dacron prosthesis (30 mm) between the aortic root and the ascending aorta was performed; the proximal section of the tubular graft was tailored to recreate the excised right coronary sinus. The reimplantation of the native right coronary artery was not technically possible and RCA was bypassed with a saphenous graft (fig 3b). Cross clamp time was 116 minutes, cardiopulmonary bypass time was 147 minutes. Histopathologic examination of the resected aneurysmal tissue confirmed a congenital etiology, with a deficiency of elastic fibers and mucoid deposits.

The postoperative course was uneventful. The patient was discharged on the 11th postoperative day. At the one-month follow-up the patient was asymptomatic; TTE, TEE and CT showed successful repair: an aortic root and ascending aorta with normal dimensions and a normally functioning aortic valve (fig 4).

Discussions

Published data about cases with coronary insufficiency secondary to SVA is scarce. An aggressive surgical approach is recommended to prevent acute coronary obstruction. In our patient the ostium of the RCA was obstructed, therefore the antegrade flow in the RCA was absent, but the vessel had a good opacification via contralateral collaterals developed as a consequence of a long-term compression [3,4].

The natural history of SVAs is difficult to be determined because of their rarity. Without surgery, many complications can be expected: rupture with sudden cardiac death, malignant arrhythmias, aortic regurgitation and infection. As in our case, unruptured SVAs are typically asymptomatic and there are no guidelines regarding the timing of surgical intervention; we decided to operate the aneurysm because its enlargement exceeded 50% of the normal sinus size [5,6].

The non-invasive diagnosis of SVA should include a complete echocardiographic examination (TTE, TEE) with the description of its origin, continuity of the aneurysmal wall, compression or obstruction caused by the SVA, severity of valvular insufficiency (aortic and tricuspid valves). The recommended key views are: parasternal long-axis view, short axis view of the aortic root, long axis view of RVOT, apical 5-chamber view. TEE, due to the probe's proximity to the aortic root, is more sensitive than TTE in describing morphological details, such as presence of thrombus, vegetations, rupture and is more suitable for differential diagnosis (e.g. with pseudoaneurysm secondary to infective endocarditis, coronary artery aneurysm) [3,7,8].

In some cases, echocardiography may be extremely challenging and difficult because of a variable aneurysmal course with multiple possibilities of extension into several positions; therefore, it is recommended to complete the imagistic evaluation with 3D-echocardiography, cardiac CT or magnetic resonance imaging (MRI). In our case, cardiac CT demonstrated that RCA was not obstructed by thrombus but compressed by the SVA. This case is one of the very few where the main mechanism of reduced RCA flow was proven to be compression exercised by the SVA [3,4,9].

In conclusion, the combination of echocardiography (TTE, TEE, 3D-TEE) with other imaging techniques (CT, MRI, cardiac catheterisation) is recommended for an accurate assessment of SVA and a precise preoperative diagnosis.

References

1. Feldman DN, Roman MJ. Aneurysms of the sinuses of valsalva. Cardiology 2006;106:73-81.
2. Hanna MF, Malguria N, Saboo SS, et al. Cross-sectional imaging of sinus of Valsalva aneurysms: lessons learned. Diagn Interv Radiol 2017;23:339-346.
3. Zhang J, Liu Y, Liu L, Deng Y. An extracardiac unruptured right sinus of valsalva aneurysm complicated with atherothrombosis. Echo Res Pract 2016;3:K1-K6.
4. Lijoi A, Parodi E, Passerone GC, Scarano F, Caruso D, Iannetti MV. Unruptured Aneurysm of the Left Sinus of Valsalva Causing Coronary Insufficiency: Case Report and Review of the Literature. Tex Heart Inst J 2002;29:40-44.
5. Weinreich M, Yu PJ, Trost B. Sinus of valsalva aneurysms: review of the literature and an update on management. Clin Cardiol 2015;38:185-189.
6. Prifti E, Ademaj F, Baboci A, Nuellari E, Demiraj A, Thereska D. Surgical treatment of a giant unruptured aneurysm of the noncoronary sinus of Valsalva: a case report. J Med Case Rep 2016;10:252.
7. Dhawan I, Malik V, Sharma KP, Makhija N, Pangasa N. Transthoracic Echocardiography versus Transesophageal Echocardiography for Rupture Sinus of Valsalva Aneurysm. Ann Card Anaesth 2017;20:245-246.
8. Yang Y, Zhang L, Wang X, et al. Echocardiographic diagnosis of rare pathological patterns of sinus of Valsalva aneurysm. PLoS One 2017;12:e0173122.
9. Regueiro Abel M, Penas Lado M, Lopez Ciudad V, Castro Beiras A. Sinus of Valsalva aneurysm as a cause of acute myocardial infarction. Rev Esp Cardiol 2002;55:77-79.

Indian J Med Res 149, March 2019, pp 376-383
DOI: 10.4103/ijmr.IJMR_415_17

Quick Response Code:

Digital pressure in haemodialysis patients with brachial arteriovenous fistula

Alexandru Oprea[1], Adrian Molnar[1], Traian Scridon[1] & Petru Adrian Mircea[2]

[1]Department of Cardiovascular Surgery, "Niculae Stancioiu" Heart Institute & [2]Department of Gastroenterology, Emergency Clinical County Hospital, University of Medicine & Pharmacy "Iuliu Hatieganu", Cluj-Napoca, Romania

Received March 10, 2017

Background & objectives: **The pathophysiological mechanisms involved in distal pressure changes following arteriovenous fistula (AVF) creation in patients with end-stage renal disease (ESRD) are not completely understood. This study was aimed to assess digital pressure changes post-AVF creation and to identify the factors that might influence these changes in ESRD patients.**

Methods: **In this prospective study, 41 patients with ESRD underwent AVF creation. Basal digital pressure (BDP), digital brachial index (DBI), calcium, phosphorus and blood urea levels were assessed preoperatively. BDP, DBI, vein and artery diameters, and AVF blood flow were also evaluated at one and two month(s) post-AVF creation.**

Results: **Mean BDP significantly decreased from 131.64±25.86 mmHg (baseline) to 93.15±32.14 and 94.53±32.90 mmHg at one and two months post-AVF creation, respectively (P<0.001). Mean DBI significantly decreased one month post-AVF creation versus baseline (0.70±0.18 vs. 0.89±0.17 mm, P<0.001) and remained similar at two versus one month(s) postoperatively (0.70±0.23 vs. 0.70±0.18 mm). At both postoperative timepoints, no correlation between DBI decrease and increased artery and vein diameters or fistula blood flow was observed. Mean DBI difference between patients with previous ipsilateral access versus those without was not significant from pre to one month postoperatively. No correlation was observed between baseline phosphorus, calcium and blood urea nitrogen and DBI changes.**

Interpretation & conclusions: **Our findings suggest that decrease in distal pressure following AVF creation may not be influenced by the arterial remodelling degree, vein diameter or fistula flow. In uraemic patients, those with low calcium and/or increased phosphorus, no association between these parameters and DBI changes could be observed.**

Key words Arteriovenous fistula - digital pressure - haemodialysis - mineral metabolism

In patients with end-stage renal disease (ESRD) who undergo surgical arteriovenous fistula (AVF) creation to provide the vascular access necessary for renal haemodialysis, changes in digital pressure can occur following AVF creation. It has been shown that the decreased digital pressure is not consistently

associated with the clinical evidence of ischaemia[1], although in some cases, it may cause pain at rest and necrosis, leading to haemodialysis access-induced distal ischaemia (HAIDI) (also known as access-related hand ischaemia, distal hypoperfusion ischaemic syndrome or arterial steal syndrome). A better understanding of the pathophysiological mechanisms involved in HAIDI occurrence is crucial for early detection of the 'at risk' patients and it would permit adopting an early therapeutic strategy[2-4].

It has been suggested that the poor remodelling of the arterial tree of the arm combined with pressure loss at the arteriovenous anastomosis, which occurs in some patients following AVF creation, could be a cause of HAIDI occurrence[5]. However, another group has shown that the decreased digital pressure occurs immediately after the surgery, without worsening in the first month, during which period, the arterial remodelling takes place[6]. Different studies suggest that the high AVF flow may cause gradual loss of blood from the forearm arteries of the same arm and lead to decreased digital pressure, followed by peripheral ischaemia[5,7,8]. In addition, in many forearm and proximal arteriovenous access, the clinically silent reversal of lower arm arterial blood flow (defined as arterial steal) can also be observed[7,8]. However, its presence does not predict or is not necessarily correlated with HAIDI[1], and it has been shown that HAIDI occurrence is more likely related to locoreginal hypotension caused by the loss of blood pressure at AVF location, because of a disturbed blood flow pattern in the anastomotic area[5]. Occlusive arterial stenosis occurring within the arteries of the upper extremity (*i.e.* proximal arteries), as well as the distal arteriopathy caused by vascular calcification, may also be involved in HAIDI pathogenesis[9,10]. The high flow accesses have been identified as having a greater risk for HAIDI than normal flow AVFs, although a normal flow combined with atherosclerosis may lead to the same outcome[11]. van Hoek *et al*[12], using a questionnaire to achieve a better selection of patients with clinical symptoms, have observed that patients with low AVF flow may also exhibit HAIDI. Therefore, high flow is not conditional for HAIDI[7].

Changes in calcium and phosphorus metabolism in patients with ESRD are frequently encountered. Greater calcification of the coronary artery, aortic and peripheral artery atherosclerotic plaques were also observed in these patients, leading to increased cardiovascular mortality and AVF failure rate[13]. Although the hardening of the arterial walls and stenosis may be involved in the occurrence of HAIDI, the role played by the mineral metabolism changes in digital pressure variation is not known.

In our study, it was hypothesized that in ESRD patients with brachial fistula accesses, the digital pressure changes following AVF creation might be associated with the AVF flow, enlargement of the vein and artery diameters after AVF creation. Considering that ESRD patients commonly have changes in the calcium, phosphorus and blood urea nitrogen (BUN) metabolism, it was also assumed that the preoperative levels of calcium, phosphorus and BUN could be correlated with digital brachial index (DBI) changes overtime.

To test this hypothesis, digital pressure changes were assessed following AVF creation at brachial level in patients with ESRD. The association between levels of calcium, phosphorus and BUN and digital pressure changes, if any, was also evaluated.

Material & Methods

This prospective study was planned to enrol all patients with ESRD who underwent brachial AVF creation between January 8, and August 1, 2014. The study was conducted in the department of Cardiovascular Surgery of the academic hospital 'Niculae Stancioiu' Heart Institute in Cluj-Napoca, Romania. The patients included were diagnosed with ESRD in dialysis centres from seven cities in Romania, and they were referred to 'Niculae Stancioiu' Heart Institute for AVF creation. The brachial arteriovenous anastomosis was performed by a single vascular surgeon, and each patient was followed up for a period of two months after AVF creation.

The study protocol was approved by the research ethics committee of 'Iuliu Hatieganu' University of Medicine and Pharmacy, Cluj-Napoca, Romania. All patients provided the informed written consent for inclusion in the study.

The study inclusion criteria were patients diagnosed with ESRD suitable for AVF creation at brachial artery (participants with cephalic and basilic vein diameters arm >1.7 mm and brachial artery diameter >2 mm were considered eligible; criteria were established based on previously published data[14], with a slight modification); and functional AVF at four weeks after creation. Patients with brachial AVF only were included in the study, because it has been shown that the prevalence of HAIDI is more common in patients with proximal

accesses than in the ones with distal accesses[11,15]. The study exclusion criteria were patients suitable for radial AVF creation (radial artery diameter >1.5 mm and cephalic vein diameter at the forearm >1.7 mm, as suggested by previously published data[14,16]); stenosis or thrombosis of the veins planned to be used for AVF creation; concomitant diagnosis of clinical/subclinical bacterial infection, and patient declined to be included in the study.

Before AVF creation, all patients were clinically examined and Doppler ultrasonography was performed, and basal digital pressure (BDP) was measured by Laser Doppler in the limb of interest. The surgical intervention was performed through a standard technique (consisting of L-T brachiocephalic or L-T brachiobasilic fistula). At one and two months after the surgery, patients were reassessed clinically and by Doppler ultrasound, as well as with Laser Doppler.

Ultrasound evaluation of the AVF arm: The Doppler ultrasonography was performed using the NextGen LOGIQ™ ultrasound machine (PR China) with a broad-spectrum linear transducer of 7-15 MHz. Pre- and postoperatively, the vein diameters were measured in cross-section at the future anastomosis place, after applying a tourniquet to the upper third of the forearm or arm. The risk of undervaluing the size of the vein because of compression by the transducer was minimized by applying copious amounts of gel and a lower downforce. The ultrasound examination of the arteries and veins continued along its whole length, being complemented by colour Doppler sonography and spectral analysis. The size of the brachial artery was recorded in real time, grey scale, on longitudinal sections. The fistula blood flow was recorded according to Napoli recommendations[17].

Assessment of systolic DBP in AVF arm: BDP was measured in the vascular laboratory (Clinical Surgery 2) in Cluj-Napoca, Romania, using a Laser Doppler Perfusion Monitoring (LDPM) unit (Perimed's PeriFlux System 5000 version 1.70-1.79, Sweden) with the Perimed's Perisoft software for Windows programme (version 2.50 Järfälla-Stockholm, Sweden), after preliminary calibration of both LDPM and pressure measuring units. A warm environment was created, and the measurement was performed after approximately 10 min, during which the patient was asked to relax. BDP was recorded in all fingers of the hand corresponding to the limb planned to be used for AVF creation. The DBI was calculated by dividing the mean DBP to the smallest value of systolic blood pressure measured in the contralateral brachial artery, according to Sumner recommendations[18]. This index was calculated to permit digital pressure evaluation by eliminating the effect of systemic blood pressure during subsequent re-examinations. DBI was assessed preoperatively, at one and two months postoperatively. According to Valentine *et al*[19], a reduction in distal perfusion was documented if a >20 mmHg decrease in BDP was observed compared to the preoperative value.

Biochemical parameters: Blood samples (2 ml) were collected preoperatively, at one and two months after AVF creation. Calcium, phosphorus and BUN levels were measured using the Architect *c*4000 Clinical Chemistry analyzer (Abbott, Illinois, USA).

Statistical analysis: Qualitative variables were summarized as associated percentages and 95 per cent confidence intervals (95% CI, shown in brackets as lower limit and upper limit). CIs were calculated using a method similar to the one presented by Jäntschi and Bolboacã[20]. Quantitative variables were summarized as mean±standard deviation (SD) for data with normal distribution.

Comparisons between proportions were performed using the *Z* test for proportions at a significance level of 5 per cent. Comparisons of the sample means were performed using the Student's *t* test for independent samples at a significance level of 5 per cent. The variables measured at different time intervals (preoperatively, 1 month postoperatively and 2 months postoperatively) were compared by the paired two sample *t* test for means at a significance level of 1.7 per cent [$\alpha^*=\alpha/K$, where $K=k\cdot(k-1)/2$, k=number of determinations over time - in the present case 3]. A statistical significant difference was considered if $P<0.05$.

The association analysis between blood biochemical parameters and DBI was performed by Pearson correlation coefficient.

Results

A total of 115 patients with ESRD were examined clinically and by ultrasonography during the study period. Of these, 59 met the eligibility criteria for brachiocephalic or brachiobasilic AVF creation (cephalic and basilic vein diameters >1.7 mm; brachial artery diameter >2 mm), nine patients refused to be included in the study. Of the 50 patients who underwent

AVF creation, nine had non-functional AVF at one month after the surgery; so finally 41 patients were included in the current analysis.

All patients were of White Caucasian heritage, with a male:female ratio of 23:18. The difference in the proportion of man (56.1%) versus women (44%) was not significant. Their age ranged between 41 and 85 yr at the time of AVF creation. The baseline demographic characteristics and AVF type are shown in Table I. Of all patients included in the analysis, 12 (30%) were not in a haemodialysis programme and 29 (70%) were on haemodialysis through internal jugular catheter at the time of AVF creation. Of the patients on haemodialysis, 10 (24%) had an AVF on the same side with the new access and eight (20%) had an AVF on the contralateral arm, but these fistulas were non-functional.

The most common type of vascular approach was brachiocephalic AVF in 32 patients (78%, 95% CI: 63.5-90.2). Brachiobasilic AVF was performed in nine patients (22%, 95% CI: 9.8-36.5). None of the patients developed clinical symptoms of HAIDI during the conduct of the study.

Table I. Patient characteristics at baseline and arteriovenous fistula type

Category	Value (%)
Age (yr), mean±SD	62±11.26
Men	23 (56)
Women	18 (44)
Associated pathology	
Diabetes	16 (39.0)
Hypertension	36 (87.8)
Ischaemic heart disease	12 (29.3)
Peripheral artery disease	6 (14.6)
Aetiology of renal disease	
Diabetes	12 (29.3)
Chronic nephritis	20 (48.8)
Renal cancer	3 (7.3)
Polycystic disease	2 (4.9)
Kidney stones	2 (4.9)
Renovascular disease	1 (2.4)
Nephrotic syndrome	1 (2.4)
Arteriovenous fistula type	
Brachiocephalic	32 (78)
Brachiobasilic	9 (22)

Evaluation of BDP, DBI and blood vessels diameters: The preoperative mean BDP was 131.64±25.86 and significantly decreased to 93.15±32.14 and 94.53±32.90 mmHg at one and two months, respectively after AVF creation (P<0.001). No significant difference was observed between BDP values at one and two months. Reduction of BDP at one and two months postoperatively compared to preoperative value was >20 mmHg in 28 of 41 patients (68.29 %). When comparing the patients without previous dialysis access with the patients with ipsilateral haemodialysis access, no significant difference was observed between BDP preoperative values (131.87±33.65 vs. 131.51±24.83 mmHg, respectively). Similar results were obtained at one month (101.39±42.77 vs. 95.39±26.52 mmHg, respectively) and two months (104.95±25.06 vs. 105.67±24.94, respectively) postoperatively.

The mean DBI significantly decreased one month postoperatively, from 0.89±0.17 to 0.70±0.18 mm (P<0.001), and remained similar at two months postoperatively compared to one month (0.70±0.23 vs. 0.70±0.18 mm, respectively). When comparing the predialysis patients without previous dialysis access versus the patients with ipsilateral haemodialysis access, no significant difference in DBI was observed between preoperative values (0.87±0.27 vs. 0.91±0.10, respectively), one month (0.67±0.22 vs. 0.73±0.14, respectively) or two months (0.71±0.16 vs. 0.78±0.12, respectively) postoperative values.

From pre- to one and two month(s) after AVF creation, the mean brachial artery and cephalic/ basilic vein diameter significantly increased, a significant increase was also observed between the diameters at one month versus two months. Taken separately, a significant increase of vein diameter between one month and two months postoperatively was observed for the cephalic vein only (Table II). The mean cephalic vein diameter increased with 3.38±1.90 mm at one month postoperatively and 4.27±2.46 mm at two months postoperatively, while the basilic vein diameter increased with 2.26±1.43 mm and 2.11±1.70 mm, respectively. The increase of the cephalic vein diameter was significantly higher compared to the increase of the basilic vein diameter at both one and two month(s) postoperative timepoints (P=0.05 and P=0.01, respectively).

Table II. Diameters of the cephalic and/or basilic veins and brachial artery used for arteriovenous fistula creation by timepoint

Diameter (mm)	n	Timepoints and comparisons of 1M post and 2M post versus pre (mean±SD)		
		Pre	1M post	2M post
Brachial artery	41	4.35±1.18	5.36±1.01***	5.54±1.18***
Cephalic/basilic vein	41	3.10±1.21	7.02±1.53***	7.72±2.25***,†††
Cephalic vein	32	3.83±1.35	7.21±1.52***	8.10±2.21***,†††
Basilic vein	9	4.08±1.59	6.33±1.42***	6.19±1.41**

*P***<0.01, ***<0.001 compared to respective pre values; †††*P*<0.001 compared to 1M Post values
AVF, arteriovenous fistula; SD, standard deviation; Pre, before AVF creation; 1M/1M Post, 1/2 month(s) after AVF creation

An increase in the AVF's flow was observed from 1154.02±643.41 ml/min at one month postoperatively to 1178.44±653.44 ml/min at two months postoperatively. However, this increase did not reach a significance. Three patients had high flow accesses (>2000 l/ml).

No significant correlation was observed between the percentage decrease of DBI at one and two months post-AVF creation and the difference between the brachial artery diameter at one month and two months, respectively, and preoperative values, between the diameter of the cephalic/basilic veins at one and two months, respectively, and preoperative values, and the flow of the AVF at one and two months postoperatively.

No significant difference of mean DBI decrease (difference between pre- and postoperative value) was observed between patients who were not enrolled in the dialysis programme at the time of AVF creation (n=12), those already on haemodialysis (n=29). The difference in the mean DBI between patients without previous access and those with previous ipsilateral access was not significant from pre to one month postoperatively (0.19±0.31 vs. 0.18±0.16, respectively).

Evaluation of calcium, phosphorus and blood urea nitrogen (BUN) levels: The association between preoperative calcium and phosphorus levels and the occurrence of digital pressure changes was analyzed by calculating the correlation between baseline calcium and phosphorus levels (Table III) and the difference between preoperative and one month post-operative DBI. No correlation was detected between baseline phosphorus level and DBI (r=0.015), neither between calcium and DBI changes (r=−0.05). The same association was assessed between preoperative BUN and DBI, but no correlation was observed (r=0.013) (Table III).

Table III. Blood biochemical parameters and correlation with digital brachial index (DBI) at baseline (n=41)

Biological parameter	Value (mean±SD)	Pearson correlation coefficient (r)
Serum phosphorus (mg/dl)	6.22±3.42	0.015
Total calcium (mg/dl)	8.45±1.07	−0.05
Urea nitrogen (mg/dl)	142.09±61.42	0.013

Discussion

Brachiocephalic fistulas are vascular access type procedures, in which hand ischaemia is the most commonly encountered complication[12]. Prior to the development of ischaemia clinical signs, a gradual decrease of BDP and DBI may be observed in patients who underwent brachial AVF creation. In our study, though a significant decrease of BDP from baseline to one and two months after AVF creation was observed, with a mean reduction in BDP >20 mmHg in 68 per cent of patients, no acute (within 24 h), subacute (within 1 month) or chronic (>1 month) forms of HAIDI[21,22] were recorded. The follow up period in our study was until two months after AVF creation, and it could be possible for some patients to develop ischaemia signs during further follow up. In a study conducted by Valentine *et al*[19], 14 (18%) patients with mean BDP reduction of 54 mmHg from pre- to three weeks after AVF creation developed ischaemia signs. In a study conducted by Papasavas *et al*[6], at a mean BDP of approximately 150 at baseline and 112 mmHg at one month after AVF creation, six patients (17%) developed ischaemia associated-symptoms. In terms of DBI, a significant decrease of 21.3 per cent was observed at one month after AVF creation compared to baseline DBI similar to that reported by Papasavas *et al*[6]. In our study, a percentage decrease of 22.2 per cent was recorded at two months after AVF

creation. The postoperative mean DBI was 0.70±0.18 and none of the patients developed clinical signs of ischaemia. In the study conducted by Valentine *et al*[19], the postoperative mean DBI was 0.65±0.29 and 18 per cent patients (14 of 72) developed ischaemia symptoms. Papasavas *et al*[6] reported DBI values of 0.7 in patients without clinical signs of ischaemia and 0.4 in patients with clinical signs of ischaemia.

Following AVF creation, the patients' arteries undergo remodelling in response to increased parietal flow and pressure. This remodelling involves increasing the diameter of the vessel without arterial wall hypertrophy[23]. In our study, the brachial artery diameter increased significantly from 4.35±1.18 mm preoperatively to 5.36±1.01 mm at one month post after AVF creation. A failure to properly remodel arteries in diabetic patients or patients with atherosclerotic high load has been proposed as a cause of hypoperfusion[5]. In our group of patients, no significant relationship between the occurrence of digital pressure changes (evidenced by a significant decrease in DBI from baseline to 1 month and 2 months after AVF creation) and the degree of arterial remodelling was observed. This finding suggests that the change in diameter of the brachial artery cannot be regarded as an independent parameter in the development of distal hypoperfusion.

Following AVF creation, the deviation of a part of the arterial blood occurs at the arteriovenous anastomosis level towards the venous side, with low resistance circuit. It has been shown that the decreased pressure appears from approximately 20-25 cm proximal to the anastomosis[2,24,25]. Vascular resistance is inversely proportional to the diameter of the vessel. In our study, the vein diameter was increased at one month postoperatively, compared to preoperatively. In our study, no significant correlation was found between the degree of development of the vein and the decrease of DBI measured at one month or two months postoperatively. This can be explained by the development of collateral circulation that can replace blood flow to the periphery[11].

We found no significant link between decrease in digital pressure and fistula flow at one and two months after AVF creation. This result differs from those of similar studies[12]. This might be due to differences in the flow of fistulas of patients included in the studies. High-flow fistulas have been shown to increase the risk for hypoperfusion[11]. Other authors, however, using photoplethysmography for objectifying hypoperfusion, suggest that hypoperfusion is not influenced by low and medium fistula flows[12]. This phenomenon can be explained by the fact that only high flow rates (>2-2.5 l/min) cause changes in the systemic circulation. Vaes *et al*[26] found an increase in systolic or diastolic blood pressure after the temporary intraoperative clamping of the fistula, only in the case of high flow fistulas. In the same study, the systolic and diastolic blood pressure increase did not occur in patients with hypoperfusion phenomenon, these patients had low and medium flow fistulas.

No correlation was observed between DBI at baseline and the biochemical parameters changes (phosphorus, calcium and BUN). However, in patients on long-term follow up, assessment of these variables should be recommended, especially because in the ESRD, due to reduced calcium intake in the hypoproteic scheme, decreased active vitamin D and calcium ion binding by excess phosphate, hypocalcaemia may occur. This causes stimulation of parathyroid hormone (PTH) synthesis and parathyroid cell hyperplasia, ultimately leading to the appearance of secondary hyperparathyroidism. Arterial calcifications are commonly encountered in this syndrome[27], and their deposits can lead to the development of arterial stenosis of varying degrees and eventually to distal hypoperfusion. The relationship between mineral metabolism changes and the occurrence of venous and arterial calcification in patients with ESRD has been demonstrated by several authors[27-30]. Taken together, these studies have demonstrated a direct relationship between the level of phosphorus and serum calcium and increased cardiovascular mortality and thrombosis of AVFs.

Our study had several limitations. First, DBI was not measured in the contralateral arm because it was decided to compare postoperative DBI values versus preoperative DBI values of the same arm. We considered that this type of comparison would be more accurate for a long-term study (patients were followed up for two years after AVF creation) due to possible vascular pathologic changes (*e.g.* different level of calcifications, thrombosis and atherosclerotic plaques) that may occur overtime on one arm only. Comparison of DBI between the arm used for AVF creation and contralateral arm might have given us a more complete overview of the differences in digital pressure after AVF creation. Second, artery calcification was not assessed in the study because a very low number of

patients were identified by ultrasonography as having scarce calcification signs in the artery of the hand used for AVF creation and none of the patients had clinical symptoms of ischaemia. Another study limitation was that PTH levels were not measured. As per routine clinical practice, PTH levels are measured only in case of high-grade calcifications detected in the arteries. As a few patients included in this analysis had minor calcification signs, it was decided not to include PTH levels in this analysis.

In conclusion, our findings suggest that the distal blood pressure decrease following AVF creation may not be influenced by the degree of arterial remodelling, vein diameter or fistula flow. In most of the cases, DBI reduction occurs within one month after AVF creation, with no further significant decrease during the second month. In uraemic patients, those with low levels of calcium ion and/or increased levels of serum phosphorus, no association between these biochemical parameters and distal pressure changes could be observed. For the routine clinical practice, preoperative measurement of DBI does not appear to be a reliable parameter for assessing potential HAIDI development after AVF creation.

Acknowledgment: The authors thank the nephrologists, study nurses and other staff members for contributing to this study. The authors are also grateful to the 'Niculae Stancioiu' Heart Institute in Cluj-Napoca, Romania for providing local logistic support.

Financial support & sponsorship: None.

Conflicts of Interest: None.

References

1. Vaes RH, Tordoir JH, Scheltinga MR. Blood flow dynamics in patients with hemodialysis access-induced hand ischemia. *J Vasc Surg* 2013; *58* : 446-510.
2. Kopriva D, McCarville DJ, Jacob SM. Distal revascularization and interval ligation (DRIL) procedure requires a long bypass for optimal inflow. *Can J Surg* 2014; *57* : 112-5.
3. Leon C, Asif A. Arteriovenous access and hand pain: The distal hypoperfusion ischemic syndrome. *Clin J Am Soc Nephrol* 2007; *2* : 175-83.
4. Modaghegh MH, Roudsari B, Hafezi S. Digital pressure and oxygen saturation measurements in the diagnosis of chronic hemodialysis access-induced distal ischemia. *J Vasc Surg* 2015; *62* : 135-42.
5. Scheltinga MR, Bruijninckx CM. Haemodialysis access-induced distal ischaemia (HAIDI) is caused by loco-regional hypotension but not by steal. *Eur J Vasc Endovasc Surg* 2012; *43* : 218-23.
6. Papasavas PK, Reifsnyder T, Birdas TJ, Caushaj PF, Leers S. Prediction of arteriovenous access steal syndrome utilizing digital pressure measurements. *Vasc Endovascular Surg* 2003; *37* : 179-84.
7. Duncan H, Ferguson L, Faris I. Incidence of the radial steal syndrome in patients with Brescia fistula for hemodialysis: Its clinical significance. *J Vasc Surg* 1986; *4* : 144-7.
8. DeMasi RJ, Gregory RT, Sorrell KA, Wheeler JR, Snyder SO, Gayle RG, *et al.* Intraoperative noninvasive evaluation of arteriovenous fistulae and grafts. The steal study. *J Vasc Tech* 1994; *18* : 192.
9. Asif A, Gadalean FN, Merrill D, Cherla G, Cipleu CD, Epstein DL, *et al.* Inflow stenosis in arteriovenous fistulas and grafts: A multicenter, prospective study. *Kidney Int* 2005; *67* : 1986-92.
10. Derici U, El Nahas AM. Vascular calcifications in uremia: Old concepts and new insights. *Semin Dial* 2006; *19* : 60-8.
11. Tordoir JH, Dammers R, van der Sande FM. Upper extremity ischemia and hemodialysis vascular access. *Eur J Vasc Endovasc Surg* 2004; *27* : 1-5.
12. van Hoek F, Scheltinga MR, Kouwenberg I, Moret KE, Beerenhout CH, Tordoir JH, *et al.* Steal in hemodialysis patients depends on type of vascular access. *Eur J Vasc Endovasc Surg* 2006; *32* : 710-7.
13. Naves-Díaz M, Passlick-Deetjen J, Guinsburg A, Marelli C, Fernández-Martín JL, Rodríguez-Puyol D, *et al.* Calcium, phosphorus, PTH and death rates in a large sample of dialysis patients from Latin America. The CORES study. *Nephrol Dial Transplant* 2011; *26* : 1938-47.
14. Wong V, Ward R, Taylor J, Selvakumar S, How TV, Bakran A, *et al.* Factors associated with early failure of arteriovenous fistulae for haemodialysis access. *Eur J Vasc Endovasc Surg* 1996; *12* : 207-13.
15. Malik J, Tuka V, Kasalova Z, Chytilova E, Slavikova M, Clagett P, *et al.* Understanding the dialysis access steal syndrome. A review of the etiologies, diagnosis, prevention and treatment strategies. *J Vasc Access* 2008; *9* : 155-66.
16. Malovrh M. Non-invasive evaluation of vessels by duplex sonography prior to construction of arteriovenous fistulas for haemodialysis. *Nephrol Dial Transplant* 1998; *13* : 125-9.
17. Napoli M. *Echo color Doppler and vascular accesses for hemodialysis. English edition.* Milano, Italy: Wichting Editore Medical Publisher; 2011. p. 5-144.
18. Sumner DS. Nonivasive vascular laboratory assessment. In: Machleder HI, editor. *Vascular disorders of upper extremity*, 2nd ed. Mount Kisco, New York: Futura Publishing Company; 1989. p. 9-57.
19. Valentine RJ, Bouch CW, Scott DJ, Li S, Jackson MR, Modrall JG, *et al.* Do preoperative finger pressures predict early arterial steal in hemodialysis access patients? A prospective analysis. *J Vasc Surg* 2002; *36* : 351-6.
20. Jäntschi L, Bolboacă SD. Exact probabilities and confidence limits for binomial samples: Applied to the difference between two proportions. *ScientificWorldJournal* 2010; *10* : 865-78.
21. Scheltinga MR, van Hoek F, Bruijninckx CM. Time of onset in haemodialysis access-induced distal ischaemia (HAIDI) is

related to the access type. *Nephrol Dial Transplant* 2009; *24* : 3198-204.

22. Modaghegh MH, Kazemzadeh G, Pezeshki Rad M, Ravari H, Hafezi S, El-Husheimi A, *et al.* Chronic hemodialysis access-induced distal ischemia (HAIDI): Distinctive form of a major complication. *J Vasc Access* 2015; *16* : 26-30.
23. Girerd X, London G, Boutouyrie P, Mourad JJ, Safar M, Laurent S, *et al.* Remodeling of the radial artery in response to a chronic increase in shear stress. *Hypertension* 1996; *27* : 799-803.
24. Illig KA, Surowiec S, Shortell CK, Davies MG, Rhodes JM, Green RM, *et al.* Hemodynamics of distal revascularization-interval ligation. *Ann Vasc Surg* 2005; *19* : 199-207.
25. Reifsnyder T, Arnaoutakis GJ. Arterial pressure gradient of upper extremity arteriovenous access steal syndrome: Treatment implications. *Vasc Endovascular Surg* 2010; *44* : 650-3.
26. Vaes RH, Tordoir JH, Scheltinga MR. Systemic effects of a high-flow arteriovenous fistula for hemodialysis. *J Vasc Access* 2014; *15* : 163-8.
27. Duncea I, Ghervan C, Georgescu C, Valea A, Lencu C, Ilie I. *Endocrinology*, 2nd ed. Cluj-Napoca: Editura Medicala Universitara, Iuliu Hatieganu; 2011.
28. Morena M, Bosc JY, Jaussent I, Dupuy AM, Terrier N, Leray-Moragues H, *et al.* The role of mineral metabolism and inflammation on dialysis vascular access failure. *J Vasc Access* 2006; *7* : 77-82.
29. Miller PE, Tolwani A, Luscy CP, Deierhoi MH, Bailey R, Redden DT, *et al.* Predictors of adequacy of arteriovenous fistulas in hemodialysis patients. *Kidney Int* 1999; *56* : 275-80.
30. Catalano C, Davì L, Normanno M, Rizzioli E, Conz PA. Vascular calcification of the venous side of an arterious-venous fistula. *J Vasc Access* 2001; *2* : 32-4.

For correspondence: Dr Adrian Molnar, 19-21 Motilor Street, 400001, Cluj-Napoca, Romania
e-mail: adimolnar45@yahoo.com

Neutrophil-to-Lymphocyte Ratio: A Comparative Study of Rupture to Nonruptured Infrarenal Abdominal Aortic Aneurysm

Sasarman Vasile Aurelian,[1,2] Molnar Adrian,[2] Octavian Andercou,[3] Schjoth Bruno,[1] Oprea Alexandru,[2] Trifan Catalin,[2] and Bindea Dan,[2] Metz, France; and Cluj-Napoca, Roumania

Background: Neutrophil-to-lymphocyte ratio (NLR) has recently emerged as a useful predictor of cardiovascular risk and adverse outcomes. According to previous studies, an NLR >5 has the highest sensitivity and specificity for postoperative morbidity and mortality in cardiovascular disease. This study aims to evaluate the NLR in cases of infrarenal unruptured abdominal aortic aneurysm (uAAA) and ruptured abdominal aortic aneurysm (rAAA) and to assess the role of NLR as a prognostic marker of 30-day mortality in patients with uAAA and rAAA who underwent surgical repair.

Methods: This retrospective cohort study examined 255 consecutive patients with intact or ruptured infrarenal AAA who underwent elective or urgent open repair surgery within our clinic in a 10-year period. Differences in prevalence were assessed using chi-squared calculations and values greater than 5 and a *P*-value less than 0.05 were considered significant. The averages were compared using the ANOVA parameter test when the Bartlett *P*-value was greater than 0.05.

Results: The average NLR appeared to be significantly higher in the group of patients with rAAA (9.3 vs. 3.39, respectively $P < 0001$). Furthermore, NLR > 5 occurred in 77.6% of patients with rAAA but only 32.5% in patients with uAAA (odds ratio 5.085; 95% confidence interval [CI]: 3.0025–8.6145; $P < 0000.1$). In terms of the postoperative prognosis in patients with uAAA, mortality after 30 days postoperatively was considerably higher at 16.6% in patients with NLR >5 compared with 6% for patients with NLR < 5 (RR: 2.77; 95% CI: 1.020–7.55; $P < 0.045$). In the case of rAAA, mortality after 30 days was higher in patients with NLR >5 (61.44%) than those with NLR < 5 (45.83%). There was no relationship between NLR and length of hospital stay or between NLR and the maximum diameter of the AAA. There was also no difference in the NLR between genders or age groups.

Conclusions: The main findings of this study were the poor outcomes in terms of 30-day mortality for the patients presenting NLR values greater than 5 undergoing open surgical repair in both categories: infrarenal uAAA and rAAA. We also show that NLR is significantly higher among patients with rAAA and that an NLR >5 indicates a 5 times greater possibility of AAA being ruptured.

We can use this easily determinable, broadly available, and inexpensive marker to identify high-risk patients, individually, or integrated into a risk-stratification system for patients diagnosed

Conflict of interest: The authors declare that there is no conflict of interest.

[1]*Regional Hospital Center Metz-Thionville, Hôpital de Mercy, Metz, France.*

[2]*Heart Institute "Niculae Stancioiu" Cluj-Napoca, Cluj-Napoca, Roumania.*

[3]*Department of Vascular Surgery, Cluj-Napoca, Roumania.*

Correspondence to: Molnar Adrian, Heart Institute "Niculae Stancioiu" Cluj-Napoca, Cluj-Napoca 400306, Roumania; E-mail: sasa_umf@yahoo.com

Ann Vasc Surg 2019; 58: 270–275
https://doi.org/10.1016/j.avsg.2018.11.026

Manuscript received: September 5, 2018; manuscript accepted: November 9, 2018; published online: 13 February 2019

with AAA. This would help in the therapeutic management of AAA, including the avoidance of open surgery when there are prohibitive risks, instead opting for an endovascular approach.

INTRODUCTION

Abdominal aortic aneurysm (AAA) is a multifactorial degenerative disease induced by a series of etiological factors, such as hypertension, atherosclerosis, degeneration, inflammation, and congenital malformations. Literature suggests that except for congenital malformations, chronic inflammation with subsequent proteolytic degradation of the aortic wall has become a histologic hallmark for aneurysms and is considered to be one of the principal causes of aortic wall weakening and aneurysm growth.[1–5]

Previous histopathological studies have revealed that the main initial stages of AAA formation are characterized by the infiltration of the tissue with a large number of exogenous immune cells like lymphocytes, macrophages, neutrophils, mast cells, and natural killer cells, inducing a chain of inflammatory response and the upregulation of matrix metalloproteinases, key enzymes directly correlated to AAA development and progression and also responsible for the maintenance of the inflammatory loop.[6–10]

Later modifications include adventitial and medial inflammatory cell infiltration, medial atrophy, and elastin fragmentation, apoptosis of vascular smooth muscle cells, medial neoangiogenesis, and thinning of the tunica media.[11,12]

Neutrophils participate in ongoing active nonspecific inflammation through the secretion of various enzymes and mediators, including elastase, myeloperoxidase, and free-oxygen radicals. Neutrophils have also been associated with collagen remodeling. In contrast to the phagocytic and killing effects of neutrophils, lymphocytes are a marker of accelerated apoptosis, which indicates a state of immunosuppression and physiological stress.[13,14] The neutrophil-to-lymphocyte ratio (NLR) is an oxidative stress and a proinflammatory marker that represents a chronic and low-grade systemic inflammatory response. This ratio has recently emerged as a useful indicator to predict cardiovascular risk and adverse outcomes. The NLR is calculated from the counts of two different but complementary immune pathways and is likely to be less influenced by confounding factors. The NLR might also be more predictive than either parameter alone. According to the latest data, an NLR >5 has the highest sensitivity and specificity for postoperative morbidity and mortality in cardiovascular diseases.[15–17]

MATERIALS AND METHODS

This retrospective cohort study examined patients with intact or ruptured infrarenal AAA who underwent elective or urgent open repair surgery within the Clinic of Cardiovascular Surgery, "Niculae Stăncioiu" Heart Institute, Cluj-Napoca, Romania from January 2007 to January 2017. The indications for surgery were aneurysm size greater than 5.5 cm in males and 5 cm in females, symptomatic aneurysms, rapid expansion rate of the aneurysm (>5 mm in 6 months), and rupture of the aneurysm. Cases were excluded if they had incomplete clinical or paraclinical data, infectious aneurysms, a need for preoperative resuscitation, or endovascular treatment. The extracted clinical data included gender, age, size of the aneurysm, presence of hypertension, diabetes, chronic renal failure, hospitalization duration, and 30-day mortality rate.

Blood samples were collected a day preoperatively before the operation in the cases of unruptured AAA (uAAA) and the day of surgery in the cases of ruptured AAA (rAAA). NLR was calculated by dividing the absolute number of neutrophils by the number of lymphocytes. Patient comorbidities are exposed in Table I and illustrate that the population presented multiple comorbidities increasing the risk of perioperative complications.

The software EpiInfo 7.2 (CDC, Atlanta) was used to calculate the prevalence, 95% confidence intervals, averages with standard deviations, and medians. Statistical differences in prevalence were assessed by chi-squared calculations and values greater than 5 and a *P*-value less than 0.05 were considered statistically significant. The averages were compared using the ANOVA parameter test when the Bartlett *P*-value was greater than 0.05. When lower than this value, the non-parametric Kruskal-Wallis test was used. For both tests, a *P*-value of less than 0.05 was considered statistically significant.

RESULTS

A total of 255 consecutive patients who underwent open surgery for infrarenal AAA were included in the final analysis. Of these, 148 had uAAA and 107 had rAAA. The patients mean age was 68.3 ± 7.6 years, and 90.4% of the population was

Table I. Patient demographics and comorbidities

Patients, n(%)	107 (41.9%)	148 (58.1%)
Age, mean ± SD	69.4 + 8.03	67.31 + 7.26
Gender, n(%) (95% CI)		
M	89.62% (82.19–94.7)	90.97% (85.06–95.11)
F	10.38% (5.3–17.81)	9.03% (4.89–14.94)
Diameter (cm), mean ± SD	7.7 + 1.12	6.65 + 1.33
Comorbidities		
DM n (%) (95% CI)	7.62% (3.35–14.46)	18.75% (12.73–26.10)
CRI n (%) (95% CI)	19.05% (9.67–29.06)	10.42% (5.95–16.6)
AHT n (%) (95% CI)	76% (70.21–81.16)	72.89% (66.58–78.58)
Smoking history n (%) (95% CI)	24% (18.84–29.79)	27.11% (21.42–33.42)
NLR, median(IQR)	9.3 (7.55–11.39)	3.39 (2.96–4.32)
30-d Mortality n (%) (95% CI)		
NLR<5	45.83% (38.34–52.35)	6% (3.86–8.89)
NLR>5	61.44% (57.25–69.35)	16.6% (12.48–20.76)

SD, standard deviation; n (%) (95% CI), number (percentage with 95% confidence interval) of patients included in a given category; DM, Diabetes mellitus; AHT, arterial hypertension; CRI, chronic renal insufficiency; IQR, interquartile range.

male. The average size of AAA was 6.84 cm with a mean of 6.65 cm for unruptured category and 7.7 cm for rAAA. A total of 7.6% of the total population had an aneurysm diameter less than 5.5 cm, of which 31.05% were female.

We compared NLR values between patients with ruptured and unruptured aneurysms, and the median NLR was higher among patients with rAAA [9.3 (IQR: 7.55–11.39) vs. 3.39 (IQR: 2.96–4.32), respectively; $P < 0001$] (Fig. 1). Similarly, the distribution of patients according to NLR was different, with NLR >5 in 77.6% of rAAA patients and NLR <5 in only 22.4%. In the case of unruptured aneurysms, 32.5% had NLR >5 and 67.5% had NLR <5 (OR 5.085; 95% CI: 3.0025–8.6145, $P < 0000.1$) (Fig. 2). This indicates a 5 times greater possibility of AAA being ruptured in the case of NLR >5.

In terms of the postoperative prognosis in uAAA patients, the mortality after 30 days postoperatively was significantly higher at 16.6% in patients with NLR >5 compared to 6% in patients with NLR <5 (RR: 2.77, 95% CI: 1.020–7.55, $P < 0.045$) (Fig. 3). The risk of mortality in AAA patients was almost 3-times higher after open surgery than in patients with NLR <5 preoperatively. In the case of rAAA, although mortality after 30 days was higher in patients with NLR >5 (61.44%) compared to those with NLR < 5 (45.83%), this difference did not reach statistical significance ($P = 0.08$). A possible explanation could be the uneven distribution of patients within the two categories. There was no relationship between NLR and the length of hospital stay or between NLR and the maximum diameter of the AAA. In addition, there was no correlation in the NLR between genders or age groups.

DISCUSSION

The main findings of this study were the poor outcomes in terms of 30-day mortality for the patients presenting NLR values greater than 5 undergoing open surgical repair in both categories: infrarenal uAAA and rAAA. We also show that NLR is significantly higher among patients with rAAA and that an NLR >5 indicates a 5 times greater possibility of AAA being ruptured.

In recent literature, there has been increasing interest in NLR as an independent marker of mortality and morbidity in cardiovascular diseases. High NLR values are associated with negative prognosis after coronary artery bypass grafting, percutaneous coronary interventions, acute aortic dissections, and peripheral vascular surgery.[6,18–22] Appeleton[15] and Kordzadeh et al.[16] studied the predictability and applicability of NLR in cases of uAAA and rAAA. These authors concluded that a preoperative NLR >5 represents an increased risk of postoperative mortality in cases of uAAA and morbidity in the case of rAAA. To our knowledge, the present study is the first to compare head-to-head NLR values and the evolution of patients according to NLR in cases of uAAA and rAAA treated by open surgery in the same surgical center with the same demographic population.

Despite the increased rate of early diagnosis and early approaches of aortic aneurysm pathology, the incidence of rAAA is increasing, accounting for about 2% of all deaths and representing the third most common cause of cardiovascular mortality after myocardial infarction and stroke.[23] Less than 50% of patients with RAAA are hospitalized, of which 30–70% die despite treatment.[24–26] The desire to

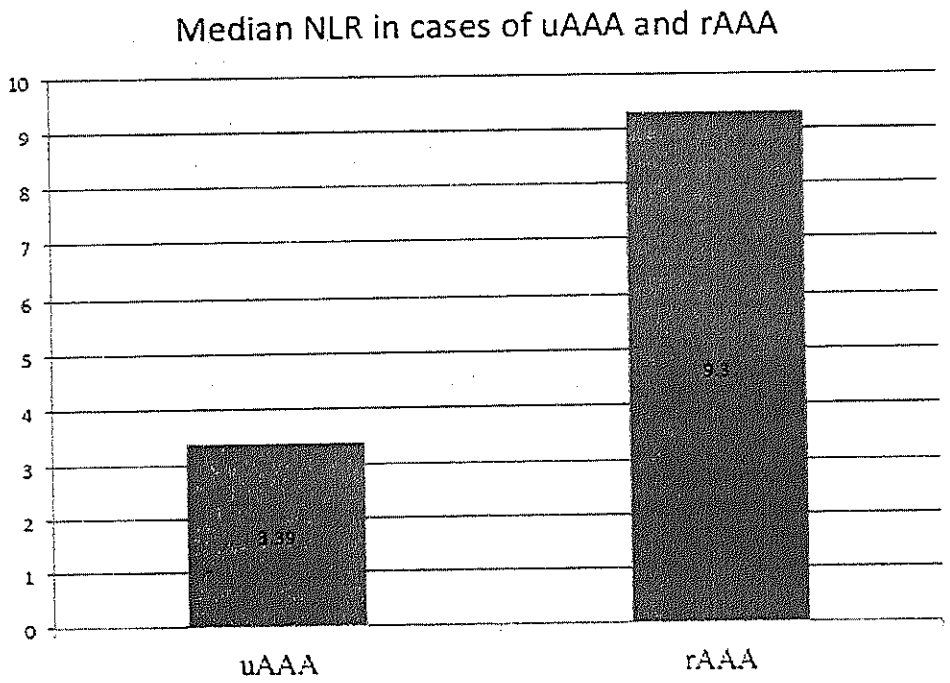

Fig. 1. Comparison between the median values of the neutrophil-to-lymphocyte ratio in the cases of unruptured and ruptured abdominal aortic aneurysms.

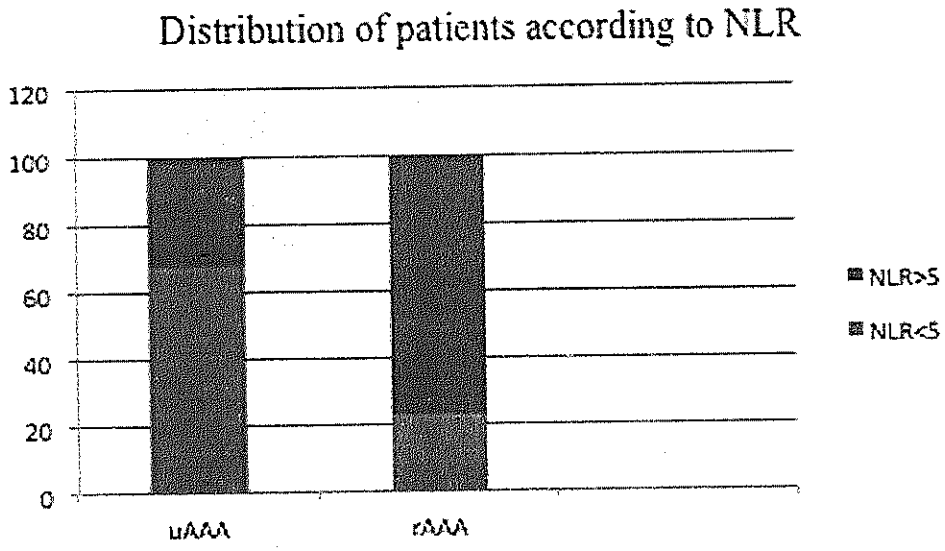

Fig. 2. The distribution of patients according to the neutrophil-to-lymphocyte ratio in the cases of unruptured and ruptured abdominal aortic aneurysms.

identify high-risk patients has led to the formulation of predictive statistical systems of mortality, such as the Glasgow Aneurysm Score, Hardman Index, Vancouver Score, Edinburgh Ruptured Aneurysm Score, University of Washington Ruptured Aneurysm Score, and Vascular Study Group of New England rAAA Risk Score. However, Thompson,[27] Gatt,[28] and Tambyraja et al.[29] have shown that these risk systems are poor predictors of the consequences after open repair surgery for AAA, with doubtful clinical application and poor correlation between them. These authors also expressed the need for a new risk classification system for patients with AAA. It is clear that NLR is an independent predictor of mortality,[15–17] as we have shown in our study. Strangely, however, it is not included in the formulas of predictive models of AAA, and none of these models assess the systemic inflammatory response.

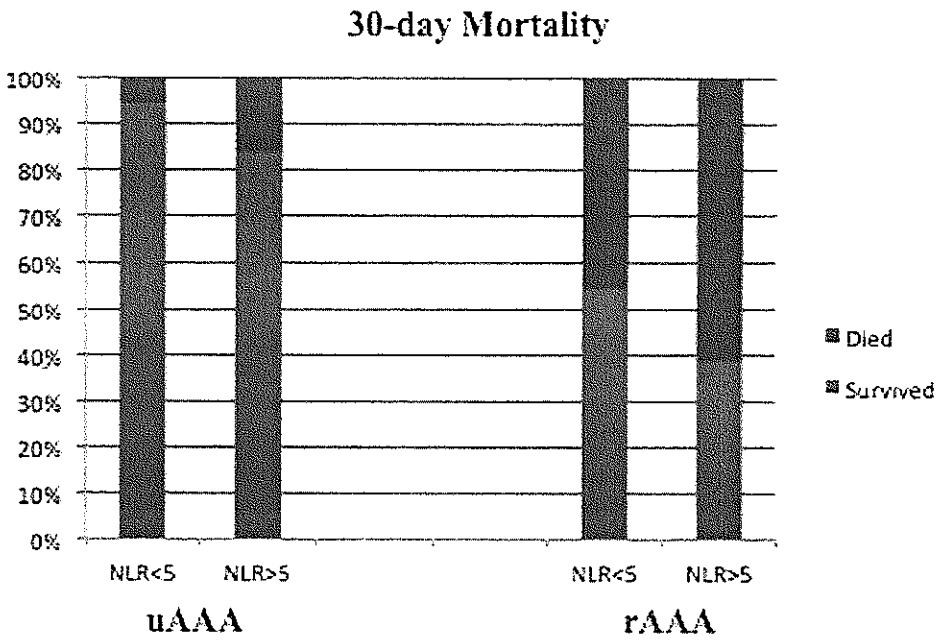

Fig. 3. The relationship between and 30-day mortality in those with a preoperative neutrophil-to-lymphocyte ratio greater or less than 5 in the cases of unruptured abdominal aortic aneurysms.

CONCLUSIONS

Our findings are in line with previous studies from the literature, which suggest that NLR >5 as a marker of chronic low-grade inflammation, which has been significantly linked to elevated 30-day mortality in cases of open surgery for AAA. These findings could be valuable for accurate assessment of patients with AAA based on mortality risk as an adjuvant factor for the choice of therapeutic management, including the avoidance of open surgery when there are prohibitive risks, instead opting for an endovascular approach. We can use this easily determinable, broadly available, and inexpensive marker to identify high-risk patients, either individually or by integration into a risk-stratification system as a pragmatic approach for mortality prediction after AAA open surgery.

REFERENCES

1. Tulamo R, Frösen J, Hernesniemi J, et al. Inflammatory changes in the aneurysm wall: a review. J Neurointerv Surg 2010;2:120–30.
2. Raffort J, Lareyre F, Clément M, et al. Monocytes and macrophages in abdominal aortic aneurysm. Nat Rev Cardiol 2017;14:457–71.
3. Cafueri G, Parodi F, Pistorio A, et al. Endothelial and smooth muscle cells from abdominal aortic aneurysm have increased oxidative stress and telomere attrition. PLoS One 2012;7: e35312.
4. Nagase H, Visse R, Murphy G. Structure and function of matrix metalloproteinases and TIMPs. Cardiovasc Res 2006;69:562–73.
5. Dale MA, Ruhlman MK, Baxter BT. Inflammatory cell phenotypes in AAAs: their role and potential as targets for therapy. Arterioscler Thromb Vasc Biol 2015;35:1746–55.
6. Haumer M, Amighi J, Exner M, et al. Association of neutrophils and future cardiovascular events in patients with peripheral artery disease. J Vasc Surg 2005;41:610–7.
7. Forester ND, Cruickshank SM, Scott DJA, et al. Increased natural killer cell activity in patients with an abdominal aortic aneurysm. Br J Surg 2006;93:46–54.
8. Eliason JL, Hannawa KK, Ailawadi G, et al. Neutrophil depletion inhibits experimental abdominal aortic aneurysm formation. Circulation 2005;112:232–40.
9. Longo GM, Xiong W, Greiner TC, et al. Matrix metalloproteinases 2 and 9 work in concert to produce aortic aneurysms. J Clin Invest 2002;110:625–32.
10. Longo GM, Buda SJ, Fiotta N, et al. MMP-12 has a role in abdominal aortic aneurysms in mice. Surgery 2005;137: 457–62.
11. Ailawadi G, Moehle CW, Pei H, et al. Smooth muscle phenotypic modulation is an early event in aortic aneurysms. J Thorac Cardiovasc Surg 2009;138:1392–9.
12. Aurelian SV, Adrian M, Dan B, et al. Giant infrarenal aortic aneurysm rupture Preceded by Left lower Limb Motor Deficit. Ann Vasc Surg 2017;43:317.e11–4.
13. Tsuruda T, Kato J, Hatakeyama K, et al. Adventitial mast cells contribute to pathogenesis in the progression of abdominal aortic aneurysm. Circ Res 2008;102:1368–77.
14. Tieu BC, Lee C, Sun H, et al. An adventitial IL-6/MCP1 amplification loop accelerates macrophage-mediated vascular inflammation leading to aortic dissection in mice. J Clin Invest 2009;119:3637–51.
15. Appleton ND, Bailey DM, Morris-Stiff G, et al. Neutrophil to Lymphocyte Ratio Predicts Perioperative Mortality Following Open Elective Repair of Abdominal Aortic Aneurysms. Int J Cardiol Heart Vessel 2014;4:30–4.
16. Kordzadeh Ali, Malietzis George, Browne Tom, et al. Neutrophil to lymphocyte ratio (NLR) of five predicts

30-day morbidity in ruptured abdominal aortic aneurysms (rAAA): a retrospective cohort study. Int J Surg 2015;15: 45–8.
17. Tan TP, Arekapudi A, Metha J, et al. Neutrophil-lymphocyte ratio as predictor of mortality and morbidity in cardiovascular surgery: a systematic review. ANZ J Surg 2015;85:414–9.
18. Papa A, Edmin M, Passino C, et al. Predictive value of elevated neutrophil-lymphocyte ratio on cardiac mortality in patients with stable coronary artery disease. Clin Chim Acta 2008;395:27–31.
19. Gibson PH, Croal BL, Cuthbertson BH, et al. Preoperative neutrophil-lymphocyte ratio and outcome from coronary artery bypass grafting. Am Heart J 2007;154:995–1002.
20. Onuk T, Güngör B, Karataş B, et al. Increased neutrophil to lymphocyte ratio is associated with in- hospital mortality in patients with aortic dissection. Clin Lab 2015;61:1275–82.
21. Kalkan ME, Kalkan AK, Gündeş A, et al. Neutrophil to lymphocyte ratio:a novel marker for predicting hospital mortality of patients with acute type A aortic dissection. Perfusion 2017;32:321–7.
22. Sbarouni E1, Georgiadou P, Analitis A, et al. High neutrophil to lymphocyte ratio in type A acute aortic dissection facilitates diagnosis and predicts worse outcome. Expert Rev Mol Diagn 2015;15:965–70.
23. Office of Population Census and Surveys, Mortality Statistics: Cause, England and Wales 1993. London: HMSO, 1995.
24. Marty-Ane CH, Alric P, Picot MC, et al. Ruptured abdominal aortic aneurysm: influence of intraoperative management on surgical outcome. J Vasc Surg 1995;22:780–6.
25. Chen JC, Hildebrand HD, Salvian AI, et al. Predictors of death in nonruptured and ruptured abdominal aortic aneurysms. J Vasc Surg 1996;24:614–23.
26. Norman PE, Jamrozik K, Lawrence-Brown MM, et al. Population based randomised controlled trial on impact of screening on mortality from abdominal aortic aneurysm. BMJ 2004;329:1259–62.
27. Thompson PC, Dalman RL, Harris EJ, Chandra V, Lee JT, Mell MW. Predictive models for mortality after ruptured aortic aneurysm repair do not predict futility and are not useful for clinical decision making. J Vasc Surg 2016;64: 1617–22.
28. Gatt M, Goldsmith P, Martinez M, et al. Do scoring systems help in predicting survival following ruptured abdominal aortic aneurysms? Ann R Coll Surg Engl 2009;91:123–7.
29. Tambyraja AL, Fraser SC, Murie JA, et al. Validity of the Glasgow Aneurysm Score and the Hardman Index in predicting outcome after ruptured abdominal aortic aneurysm repair. Br J Surg 2005;92:570–3.

Ahead of print

Med Ultrason 2020:0, 1-4 Online first
DOI: 10.11152/mu-2325

The role of multimodal imaging in the diagnosis of an asymptomatic patient with congenital anomaly

Raluca Tomoaia[1,2], Adrian Molnar[1,2], Ruxandra Ștefana Beyer[1], Alexandra Dădârlat-Pop[1,2], Florina Frîngu[2,3], Diana Gurzău[2,3], Gelu Simu[2,3], Ioan Alexandru Minciună[3], Bogdan Caloian[2,3], Dumitru Zdrenghea[2,3], Dana Pop[2,3]

[1]"Niculae Stancioiu" Heart Institute, [2]"Iuliu Haţieganu" University of Medicine and Pharmacy, [3]Clinical Rehabilitation Hospital, Cardiology Department, Cluj-Napoca, România

Abstract

Anomalous left coronary artery from the pulmonary artery (ALCAPA) syndrome is a rare congenital coronary anomaly, which can cause potentially fatal complications, such as heart failure, myocardial infarction and sudden cardiac death. Only a few patients left untreated survive to adulthood. We highlight the importance of multimodal imaging in the diagnosis of ALCAPA syndrome in a young asymptomatic female patient with inducible ischemia on exercise. The patient was successfully treated with surgery.

Keywords: multimodal imaging; ALCAPA; coronary angiography; echocardiography

Introduction

Anomalous left coronary artery from the pulmonary artery (ALCAPA) syndrome is a rare congenital anomaly, affecting 1 of 300.000 newborns. Approximately 90% of patients die during the first year of life due to myocardial infarction and heart failure. The rest of the cases (18-25%) develop sufficient myocardial collaterals between the anomalous left coronary artery and the normal right coronary artery and manage to survive to adulthood. This compensatory mechanism leads to a left to right shunt to the pulmonary artery, with coronary steal phenomenon, resulting in the development of myocardial ischemia, arrhythmias and heart failure later in life. Treatment of ALCAPA syndrome includes several surgical techniques, all associated with an increased morbidity [1]. We report the case of an asymptomatic 24-year-old female patient referred to our center for cardiology evaluation before joining the national basketball team. She was diagnosed with ALCAPA syndrome and was managed surgically with good outcome.

Received 28.11.2019 Accepted 02.02.2020
Med Ultrason
2020:0 Online first, 1-4
Corresponding author: Adrian Molnar MD, PhD
"Niculae Stancioiu" Heart Institute
19-21, Moţilor street,
400001, Cluj-Napoca, Romania
Phone: +40264597256
E-mail: adimolnar45@yahoo.com

Case report

A 24-year-old previously asymptomatic female patient was referred to our cardiology department for evaluation before joining the national basketball team. She denied any history of palpitations, angina or dyspnea and had no family history of sudden cardiac death (SCD). There were no pathological findings on clinical examination. Electrocardiogram revealed diffuse ST-T changes. The exercise stress test showed further ST depression (up to 5 millimeters), which was predominant in V2-V6.

Routine transthoracic echocardiography (TTE) revealed multiple turbulent flows in the interventricular septum and in the lateral left ventricular (LV) wall, both in systole and diastole (fig 1A-D). There was also a significant thickening of the lateral LV wall, which was not dilated and had a preserved global systolic function (fig 1E),

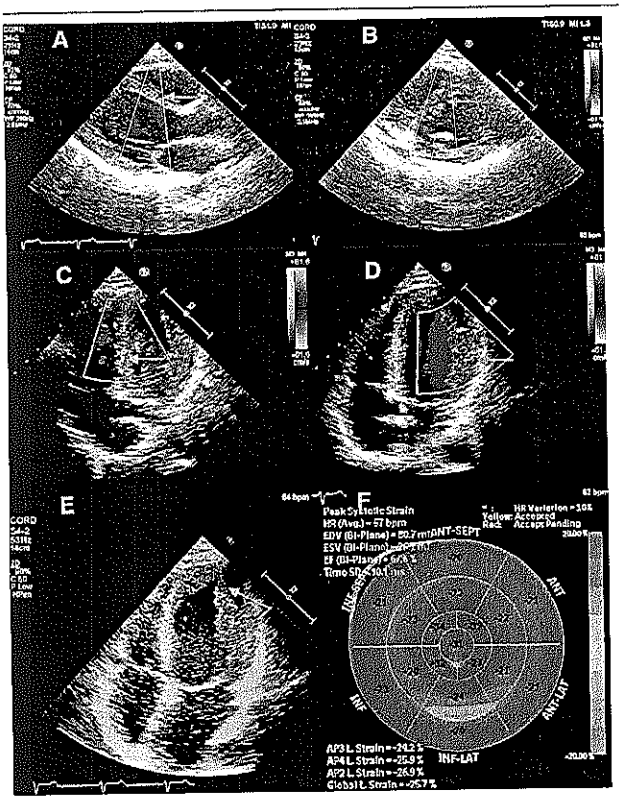

Fig 1. TTE showing multiple turbulent flows (arrows) in the interventricular septum from parasternal long (A) and short (B) axis. Same findings (arrows) from apical 4 chamber view in the interventricular septum (C) and in the lateral LV wall (D). Apical 4chamber view revealing significant thickening (arrows) of the lateral LV wall (E). Bulls-eye showing reduced regional longitudinal strain at the level of the lateral wall (F).

but with reduced regional longitudinal strain at the level of the lateral wall (fig 1F). Therefore, the suspicion of multiple ventricular septal (VSD) defects was raised, possibly associated with left ventricular noncompactation (LVNC).

Magnetic resonance imaging (MRI)was afterwards performed, with visualization of a LV with preserved ejection fraction and sub-endocardial late gadolinium enhancement (LGE) at the level of the lateral and anterior septal LV walls. MRI criteria for LVNC were also positive (Petersen index of 4.4 at the level of the apex, 2.6 at the level of the lateral wall). Furthermore, there were multiple millimetric lodges within the myocardium, predominantly at the level of the same LV walls (fig 2). Thus, a coronary anomaly was suspected and a coronary computed tomography angiography (CCTA) was considered necessary as a next step.

CCTA revealed giant coronary arteries (CA) - the left CA (LCA) measured 10.3 mm, the left anterior descending CA (LAD) 7.4 mm and the right CA (RCA) 8.8 mm. There was an anomalous origin of the LCA from the pulmonary artery (PA), with a normal origin of the RCA and many myocardial collaterals between the LAD and the RCA (fig 3).

Subsequently the patient underwent cardiac surgery with ligation of the proximal segment of the anomalous LCA and grafting of the left internal mammary artery into the distal segment of the artery. Two months later, the follow-up echocardiography revealed a significant reduction of the collateral vessels (fig 4). The patient decided to postpone joining the basketball team at that moment.

Discussion

ALCAPA syndrome is a very rare congenital disease and accounts for 0.25-0.5% of all congenital heart defects [1]. Survival is a rare finding in the adult population, depending on the development of inter-coronary collaterals between the left and the right CA. The left-to-right shunt leads to coronary steal phenomenon, with low oxygenation of the lateral left ventricular (LV) wall as a consequence of preferential flow of the blood to the low-pressure PA as opposed to the myocardium. This mechanism may cause chronic myocardial ischemia and myocardial infarction, leading to malignant arrhythmias and SCD [2]. Once ALCAPA is diagnosed, surgery should be performed immediately [3].

Electrocardiography may raise the suspicion of this anomaly in a young adult, showing ischemic changes (most frequently negative T waves in DI and aVL) [4], which were also present in our patient.

Even though coronary artery angiography was the gold standard for the diagnosis of ALCAPA syndrome, noninvasive imaging is sufficient in the modern era [3]. Echocardiography may visualize a dilated RCA, retro-

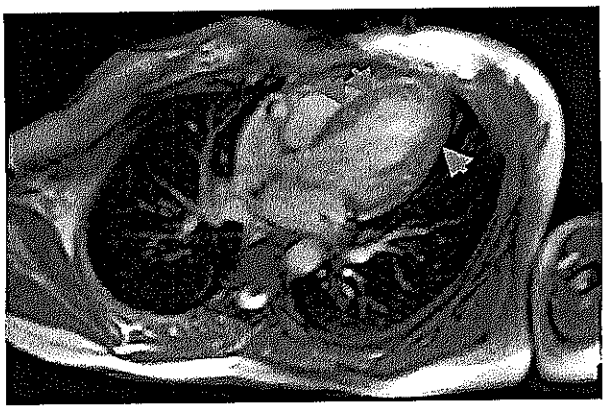

Fig 2. MRI visualizing multiple millimetric lodges within the myocardium, predominantly at the level of the septum and lateral LV wall (arrows).

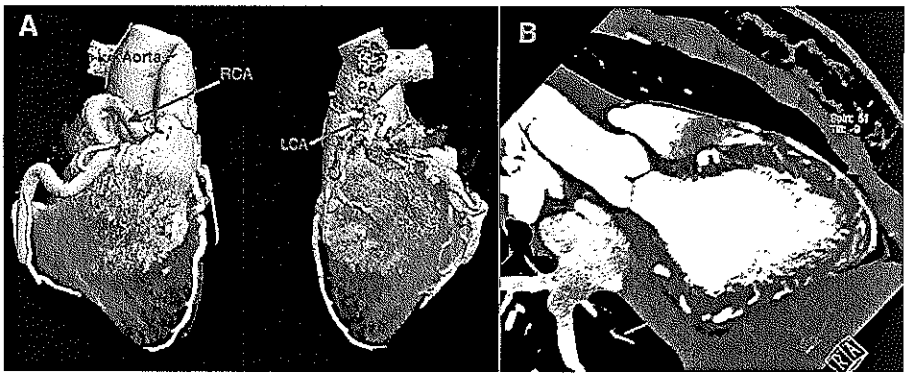

Fig 3. CCTA revealing an anomalous origin of the LCA from the PA with a normal origin of the RCA(A) and many collaterals (red arrows) between LAD and RCA (B).

grade flow from the LCA to the PA and the collaterals with systolic and diastolic blood flow [5]. Moreover, speckle tracking echocardiography reveals reduced longitudinal and circumferential strain in the regions corresponding to the LCA [2]. CCTA allows excellent spatial resolution to establish the origin and course of the CA [2]. MRI can be useful due to the benefit of LGE, which indicates fibrosis secondary to chronic ischemia [6]. Some of these findings were also present in our patient. There were septal and lateral color flow signals on echocardiography, with reduced regional strain at the level of the lateral LV wall. The CCTA revealed the abnormal course of the RCA with anastomoses between the right and left CA. MRI demonstrated fibrosis at the level of the lateral and anterior septal walls as a sign of chronic ischemia.

The connection between ALCAPA syndrome and LVNC can be explained by early embryonic development. ALCAPA is the result of abnormal septation of the conotruncus into the aorta and pulmonary artery or due to persistence of the pulmonary buds and involution of the aortic buds. On the other hand, LVNC is caused by the arrest of the embryogenesis of the endocardium and myocardium, with coronary circulation being developed simultaneously during this process, when intratrabecular recesses are reduced to capillaries [2]. In our patient, both echocardiography and MRI showed a thickened lateral LV wall with positive criteria of LVNC, but with multiple milimetric lodges inside the myocardium, demonstrating the connection between the two processes (development of the CA and compactation of the LV).

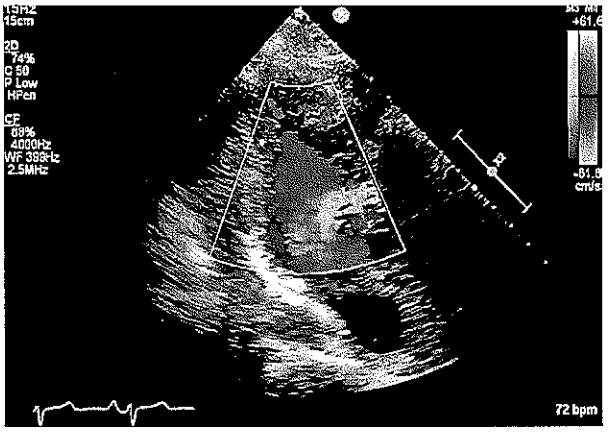

Fig 4. Three-months postoperative TEE showing significant reduction of the collateral vessels.

If untreated, ALCAPA syndrome has a high mortality (80-90%) [2]. SCD occurs mainly in young athletes and basketball players [1]. A literature review of 151 patients with this pathology found that 14% were asymptomatic and 62% of those with SCD were asymptomatic before the diagnosis was established [7].

The particularity of our case consists in the rarity of survival in patients with ALCAPA syndrome when left untreated, moreover with the patient being asymptomatic and physically active. Even though ALCAPA is rare in the adult population, the diagnosis is essential since early treatment may prevent myocardial damage. Current guidelines indicate that such patients may return to competitive sports 3 months postoperatively, provided that they remain asymptomatic and an exercise stress test does not show ischemia or important arrhythmias [3].

In conclusion we underline the importance of imaging in the early diagnosis of patients with ALCAPA syndrome. Furthermore, we highlight the connection between CA anomalies and LVNC, as these two processes coincide during early embryogenesis.

References

1. Harmon KG, Asif IM, Maleszewski JJ, et al. Incidence, cause, and comparative frequency of sudden cardiac death in national collegiate athletic association athletes: a decade in review. Circulation 2015;132:10-19.

2. Elumalai G, Sujitha AS. "Anomalies origin of left coronary artery" its embryological basis and clinical significance. Elixir Embryology 2016;100:43446-43449.
3. Brothers JA, Frommelt MA, Jaquiss RDB, Myerburg RJ, Fraser CD, Tweddell JS. Expert Consesnsus guidelines: Anomalous aortic origin of a coronary artery. J Thorac Cardiovasc Surg 2017;153:1440-1457.
4. Dilawar M, Ahmad Z. Anomalous left coronary artery from pulmonary artery: Case series and brief review. OJPed 2012;2:77-81.
5. Patel SG, Frommelt MA, Frommelt PC, Kutty S, Cramer JW. Echocardiographic diagnosis, surgical treatment, and outcomes of anomalous left coronary artery from the pulmonary artery. J Am Soc Echocardiogr 2017;30:896-903.
6. Boutsikou M, Shore D, Li W, et al. Anomalous left coronary artery from the pulmonary artery (ALCAPA) diagnosed in adulthood: Varied clinical presentation, therapeutic approach and outcome. Int J Cardiol 2018;261: 49-53.
7. Memon MKY, Amanullah M, Atiq M. Anomalous Left Coronary Artery from Pulmonary Artery: An Important Cause of Ischemic Mitral Regurgitation in Children. Cureus 2019;11:e4441.

medicina

MDPI

Case Report

Gastric Adenocarcinoma Associated with Acute Endocarditis of the Aortic Valve and Coronary Artery Disease in a 61-Year-Old Male with Multiple Comorbidities—Combined Surgical Management—Case Report

Horaţiu Moldovan [1,2], Daniela Popescu [3], Teodor Buliga [4], Anca Filip [5], Iulian Antoniac [6], Daniela Gheorghiţă [6,*] and Adrian Molnar [7]

1 Department of Cardiovascular Surgery, Sanador Hospital, 010991 Bucharest, Romania; h_moldovan@hotmail.com
2 Titu Maiorescu University, Faculty of Medicine, 004051 Bucharest, Romania
3 Department of Cardiology, Sanador Hospital, 010991 Bucharest, Romania; dani31popescu@yahoo.com
4 Department of General Surgery, Sanador Hospital, 010991 Bucharest, Romania; teodorbuliga@yahoo.com
5 Department of Intensive Care, Sanador Hospital, 010991 Bucharest, Romania; anca.filip@sanador.ro
6 University Politehnica of Bucharest, Faculty of Materials Science and Engineering, 060042 Bucharest, Romania; antoniac.iulian@gmail.com
7 Iuliu Hatieganu University of Medicine and Pharmacy, 400129 Cluj–Napoca, Romania; adimolnar45@yahoo.com
* Correspondence: daniela.mgm8@gmail.com

Received: 27 February 2019; Accepted: 24 May 2019; Published: 3 June 2019

Abstract: The case of a 61-year-old male with a recent total gastrectomy for a hemorrhagic gastric tumor is presented, with the important co-morbidities of type II diabetes mellitus requiring insulin, chronic hepatitis C with liver dysfunction, stage II essential hypertension, chronic stage III renal disease peripheral type II aorto-iliac disease with stage II ischemia of both legs, and chronic anemia. About one month following the gastrectomy, the patient presented with fever and acute inflammatory syndrome. Severe aortic insufficiency, aortic valvular vegetations, and positive blood cultures with Staphylococcus saprophytic were found. The diagnosis of infectious endocarditis on the aortic valve was established (positive blood cultures with echocardiographic features of vegetations, fever), and antibiotic treatment with Levofloxacin and Vancomycin was initiated. The evolution was favorable with the remission of the inflammatory syndrome and quick cessation of fever. However, the hemodynamic aspect showed progressive heart failure with acute pulmonary edema. The transesophageal echocardiographic examination confirmed the existence of severe aortic insufficiency and valvular vegetations with a left ventricular ejection fraction of 38%. The coronary angiography revealed double vessel disease. The calculated Euroscore II was 33.4%. Aortic valve replacement with porcine xenograft and double coronary artery bypass graft surgery was performed. The patient had a favorable postoperative course remaining afebrile and out of heart failure, with the markers of inflammation largely within normal limits. The left ventricular ejection fraction increased to 50%. The successful outcome of this case, represented by a rare association of cancer, endocarditis, and coronary disease, reveals the importance of the multidisciplinary teams involved in this case: gastroenterology, general surgery, cardiology, infectious diseases, cardiac surgery, and intensive care. Therefore, in such cases with high risk, complex patients, a strong collaboration between all specialties is needed to overcome all of the limitations of the patient's co-morbidities.

Keywords: gastric tumor; gastrectomy; aortic valve endocarditis; acute pulmonary edema; double coronary lesions

1. Introduction

This case report has a cardiological aspect, presenting a rare association between cancer and two cardiological aspects (coronary disease and endocarditis). Abdominal surgery complications were related in this case to cancer disease, that through its definition affects the immune system. With the immune system affected and preexistent co-morbidities, the patient developed a paraneoplastic immune depression. Therefore, the result was an infection with Staphylococcus saprophytic that represented the precursor to valvular endocarditis.

A frail patient subjected to an extensive surgical procedure can occasionally become subject to an unforeseen and unwelcome complication such as bacterial endocarditis. From mundane dental procedures or other types of maxillofacial surgery to any other surgical intervention of the gastrointestinal tract, bacterial or fungal endocarditis can follow [1,2]. Left sided endocarditis is more frequent than right heart endocarditis. Right heart valves are more frequently affected in patients on chronic hemodialysis, intravenous drug users, and patients with implantable electronic cardiac devices [3]. Left sided endocarditis is more common in patients with major comorbidities who undergo non-cardiac major surgery [4,5].

2. Case Presentation

We present the case of a 61-year-old insulin-requiring diabetic patient with chronic C viral hepatitis, type II aorto-iliac peripheral artery disease with chronic stage II ischemia of both legs with anemia and hypovolemia who presented with a massive upper gastrointestinal tract (GIT) bleeding due to a hemorrhagic gastric adenocarcinoma. An urgent CT (computerized tomography) was performed, showing the gastric tumor (Figure 1). Based on the critical status of the initial presentation, the patient was taken to theater in emergency, where a total gastrectomy was performed (esophago-jejune-anastomosis, Omega shaped with Brown anastomosis at the tip of the jejunal loop) and the gastric adenocarcinoma surgical specimen was removed (Figure 2). After the gastrectomy procedure, the patient was closely monitored. Given the favorable evolution and lack of post-operative complications, the patient was discharged.

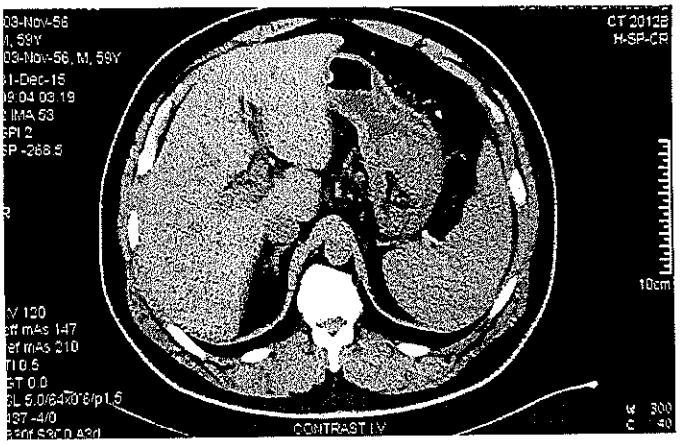

Figure 1. Computer Tomography (CT) scan showing the gastric tumor.

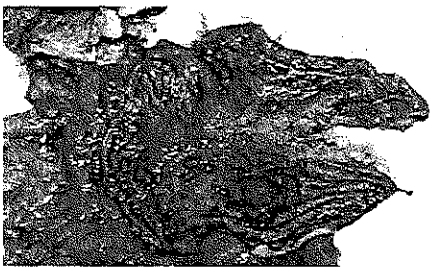

Figure 2. Surgical specimen with the gastric adenocarcinoma.

The histopathological examination revealed the presence of regional lymphangiomas, some with moderately differentiated adenocarcinoma metastasis and the rest with only a reactive aspect. The examination further revealed tumor deposits in peritumoral adipose tissue, intramural intravascular tumoral emboli, and histologically preserved epiploon, without malignant tumoral elements. Throughout the gastric mucosa, at different levels, numerous formations of sessile and semi-pediculate grayish polyploids with a histopathological appearance of tubular adenomatous polyp and tubules with light and moderate dysplasia were found. Figure 3 presents a representative image of the histopathological examination.

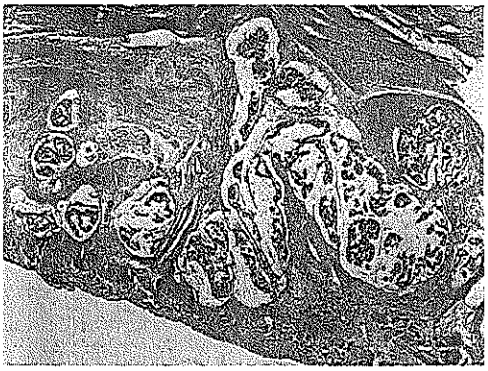

Figure 3. Histopathology examination of the gastric adenocarcinoma specimen.

After the gastrectomy, the patient underwent X-ray radiography (Figure 4). Four weeks later, the patient developed a marked inflammatory syndrome (erythrocyte sedimentation rate (ESR) 100 mm, White Cell Count (WCC) 20,000, C-Reactive Protein test (CRP) 30, raised procalcitonin test, and pyrexia). The clinical examination revealed a diastolic aortic murmur with collapsing pulses. The transthoracic ECHO detected multiple aortic leaflet vegetations with severe regurgitation (grade IV). Blood cultures identified Staphylococcus saprophytic. As there was no existence of dental infections, malnutrition, or preexistent aortic lesions, due to the cancer and preexistent co-morbidities, the patient developed a paraneoplastic immune depression that resulted in the Staphylococcus saprophytic infection.

Antibiotic treatment with IV Levofloxacin and Vancomycin was initiated, where there was a significant improvement of the inflammatory syndrome, however, the hemodynamic burden resulted in heart failure with acute pulmonary edema and recurrent episodes of myocardial ischemia at rest.

The patient was transferred to the Intensive Care Unit where he received inotropic support with Dobutamine, Levosimendan, and loop diuretics. The coronary angiogram showed a proximal critical stenosis of the left anterior descending artery (LAD) (Figure 5) and a tight lesion of the obtuse marginal (OM1) (Figure 6).

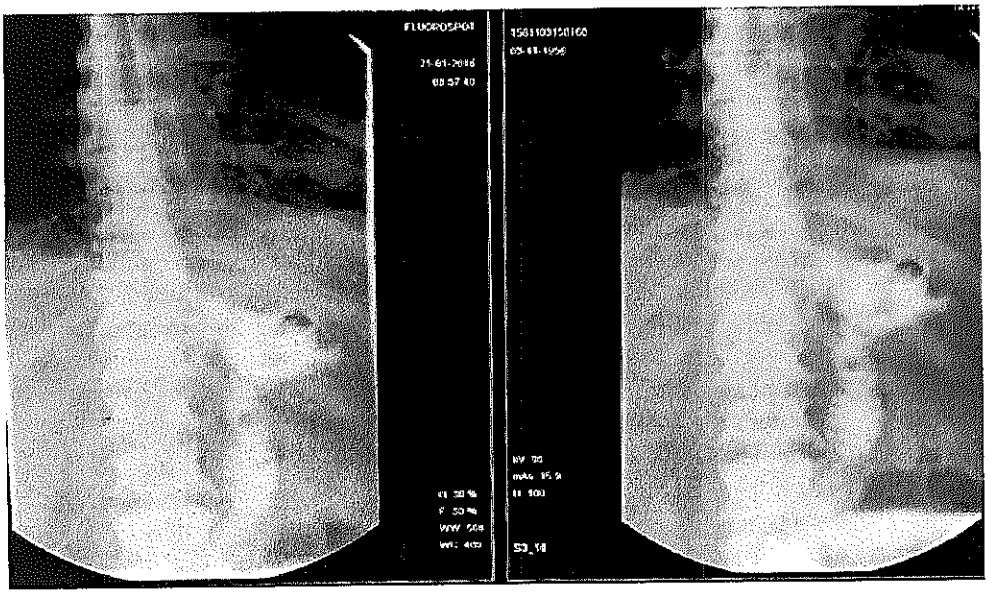

Figure 4. Radiological image after total gastrectomy and gastrojejunoanastomosis.

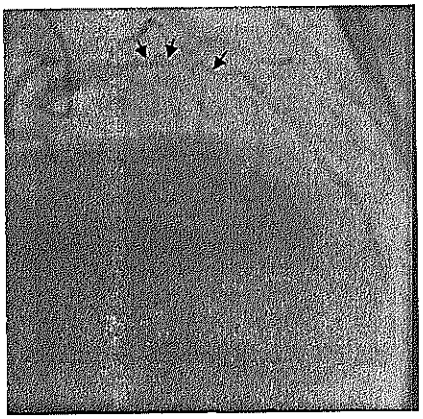

Figure 5. Left coronary angiogram - arrows show severe proximal left anterior descending artery (LAD) stenosis.

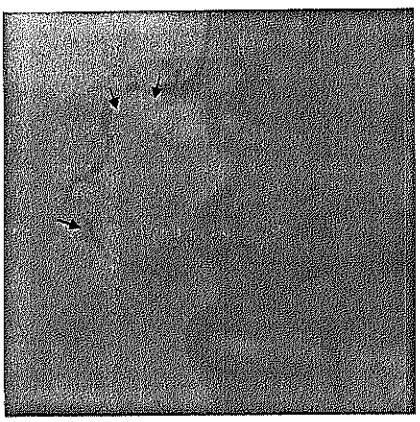

Figure 6. Right coronary angiogram - arrows show subocclusion in the second segment.

The transesophageal echocardiography (TEE) showed a hypokinetic anterior wall of the left ventricle with significant systolic dysfunction ejection fraction (EF) 38%. There was a perforated noncoronary cusp with severe aortic regurgitation and a large 20 mm vegetation (Figure 7). The calculated Euroscore II was 33.4%.

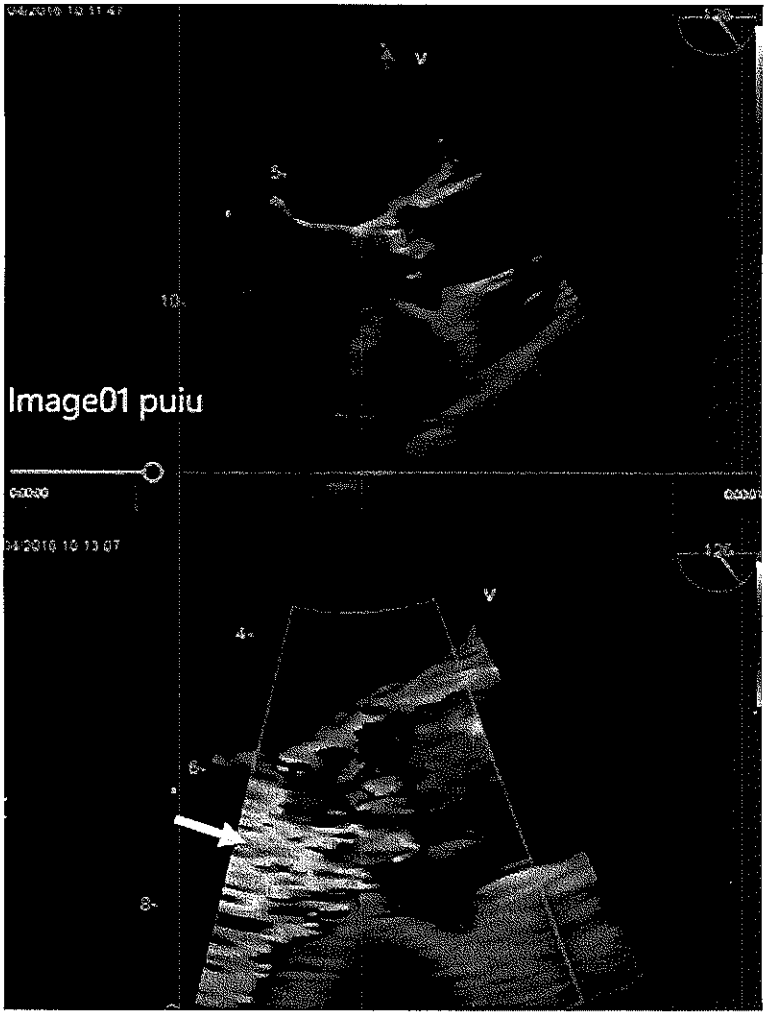

Figure 7. Echocardiographic image showing the aortic valve vegetation and aortic regurgitation.

Aortic valve replacement (21 Medtronic Hancock II porcine xenograft) (Figure 8) and double vessel coronary artery bypass graft surgery was performed: left internal mammary artery (LIMA)—LAD and saphenous vein graft (SVG)—OM1. Intraoperatively, the perforation of the noncoronary cusp was confirmed and multiple vegetations were involved in all three aortic leaflets; fortunately there was no aortic root abscess. The study was approved under ethical number 3958 by Sanador Hospital (approved on 26 May 2016). Informed consent was obtained from the participant.

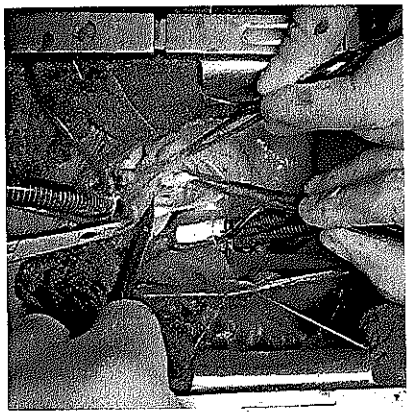

Figure 8. Surgical view of the aortic valve showing the aortic vegetation.

3. Discussion

The postoperative course was uneventful. The patient required mechanical ventilation for only 24 hours, and hemodialysis was necessary for a short period (three sessions only). Vasoconstrictor treatment with noradrenaline was continued for three days postoperatively and low dose dobutamine infusion was maintained for the entire period of stay in the Intensive Care Unit (ICU) stay.

Ten days following the cardiac surgery, the left ventricular ejection fraction increased to 45% and the inflammatory syndrome improved substantially. The patient, however, developed an extensive edematous syndrome two weeks later; hypoalbuminemia, heart failure, and inflammation could all have had a contributory factor. Diuretics, albumin infusion, and iron supplements were given and eventually the edema subsided.

The patient was discharged 18 days postoperatively in optimal conditions. The aortic prosthesis was functioning well, the left ventricular function greatly improved to a 50% ejection fraction without any sign of heart failure, there were normal levels of inflammatory markers, and no low grade pyrexia. Antibiotic treatment was continued for six weeks after surgery. The follow ups at one month, three months, and six months showed no further complications with a more than satisfactory clinical condition.

The appearance of a septic complication after cancer surgery can be represented by infectious endocarditis even if there have been no previous valvular lesions [6,7]. Usually, patients operated on for gastric cancer are closely monitored in a digestive surgery environment and the focus can resume on the abdominal sphere [8]. We therefore draw attention to a cardiac related complication after a major abdominal surgery [9,10].

4. Conclusions

Endocarditis with destruction of the aortic valve is a severe complication following major abdominal surgery for bleeding gastric adenocarcinoma. This patient had multiple co-morbidities: type II diabetes, liver dysfunction with hepatitis C, stage II essential hypertension, chronic stage III kidney disease, aortoiliac peripheral type II disease with chronic stage II ischemia of both legs, and chronic anemia.

The severity of the case was compounded by the ongoing myocardial ischemia due to critical coronary lesions (almost a left-main equivalent) and aortic regurgitation. The absence of cardiovascular symptoms before the abdominal surgery is puzzling in the context of anemia and hypovolemia. The successful outcome of this case with complex pathology is the direct result of a multidisciplinary approach where many hospital based specialties were involved.

This case report is a presentation of a rare case of cardiological complications associated with cancer. The complexity of this case is represented by the multiple diagnosis and co-morbidities that were successfully managed by the multidisciplinary team.

Author Contributions: Conceptualization, H.M. and I.A.; Methodology, H.M., D.P., T.B., A.F., I.A. and D.G.; Software, D.G. and A.M.; Validation, H.M., I.A., D.P. and A.F.; Formal analysis, H.M., I.A. and A.M.; Investigation, I.A., D.P., D.G. and A.M.; Resources, H.M., D.P., T.B., A.F., I.A., D.G. and A.M.; Data curation, H.M., T.B. and I.A.; Writing—original draft preparation, I.A., H.M., A.F. and D.G.; Visualization, T.B., A.F. and A.M.; Supervision, H.M. and I.A.; Project administration, I.A., H.M. and D.G.; Funding acquisition, I.A. and H.M.

Funding: This research was funded by a grant from the Romanian Ministry of Research and Innovation, CCCDI-UEFISCDI, project number PN-III-P1-1.2-PCCDI-2017-0239/60PCCDI 2018 within PNCDI III.

Conflicts of Interest: The authors declare no conflicts of interest.

References

1. Arbulu, A.; Asfaw, I. Management of infectious endocarditis: Seventeen years of experience. *Ann. Thorac. Surg.* **1987**, *43*, 144–149. [CrossRef]
2. Macarie, C.; Iliuta, L.; Savulescu, C.; Moldovan, H.; Gherghiceanu, D.P.; Vasile, R.; Filipescu, D.; Candea, V. Echocardiographic predictors of embolic events in infective endocarditis. *Kardiol. Pol.* **2004**, *60*, 535–540. [PubMed]
3. McKenzie, H.; Kathyrn, G.; Michele, S. 4-Valve Heart Disease and Right Heart Failure. *J. Cardiothorac. Vasc. Anesth.* **2018**, *32*, 838–845.
4. Ali, H.; Wolfgang, B.; Alexander, P.; Azita, A.R.; Bernhard , R.B.; Hans, R.F.; Thorsten, D.; Marcus, F.; Christian, J. Left atrial endocarditis as a rare complication of mitral valve endocarditis: A clinical case. *BMC Cardiovasc. Disord.* **2012**, *12*, 103.
5. Fernández-Hidalgo, N.; Almirante, B.; Tornos, P.; González-Alujas, M.T.; Planes, A.M.; Galinanes, M.; Pahissa, A. Immediate and long-term outcome of left-sided infective endocarditis. A 12-year prospective study from a contemporary cohort in a referral hospital. *Clin. Microbiol. Infect.* **2011**, *17*, 769–775.
6. Sârbu, I.; Vassu, T.; Chifiriuc, M.C.; Bucur, M.; Stoica, I.; Petrut, S.; Rusu, E.; Moldovan, H.; Pelinescu, D. Assessment the activity of some enzymes and antibiotic substances sensitivity on pathogenic bacteria species. *Rev. Chim.* **2017**, *12*, 1–23.
7. Jaffe, W.M.; Morgan, D.E.; Pearlman, A.S.; Otto, C.M. Infectious endocarditis 1983–1988, Echocardiographic findings and factors influencing morbidity and mortality. *J. Am. Coll. Cardiol.* **1990**, *15*, 1227–1233. [CrossRef]
8. Hamada, Y.; Yamada, M.; Furuno, T.; Fujii, C.; Matsumura, Y.; Yabe, T.; Seo, H.; Takata, J.; Chikamori, T.; Doi, Y. Two cases of Candida endocarditis associated with abdominal disease. *Nihon Ronen Igakkai Zasshi* **1996**, *33*, 33–37. [CrossRef] [PubMed]
9. Devereaux, P.J.; Sessler, D.I. Cardiac complications in patients undergoing major noncardiac surgery. *N. Engl. J. Med.* **2015**, *373*, 2258–2269. [CrossRef] [PubMed]
10. Tomsic, A.; Li, W.W.; van Paridon, M.; Bindraban, N.R.; de Mol, A.J.M. Infective Endocarditis of the Aortic Valve with Anterior Mitral Valve Leaflet Aneurysm. *Tex. Heart Inst. J.* **2016**, *43*, 345–349. [CrossRef] [PubMed]